IMSE

Institute for Materials Science and Engineering

FRACTURE AND DEFORMATION

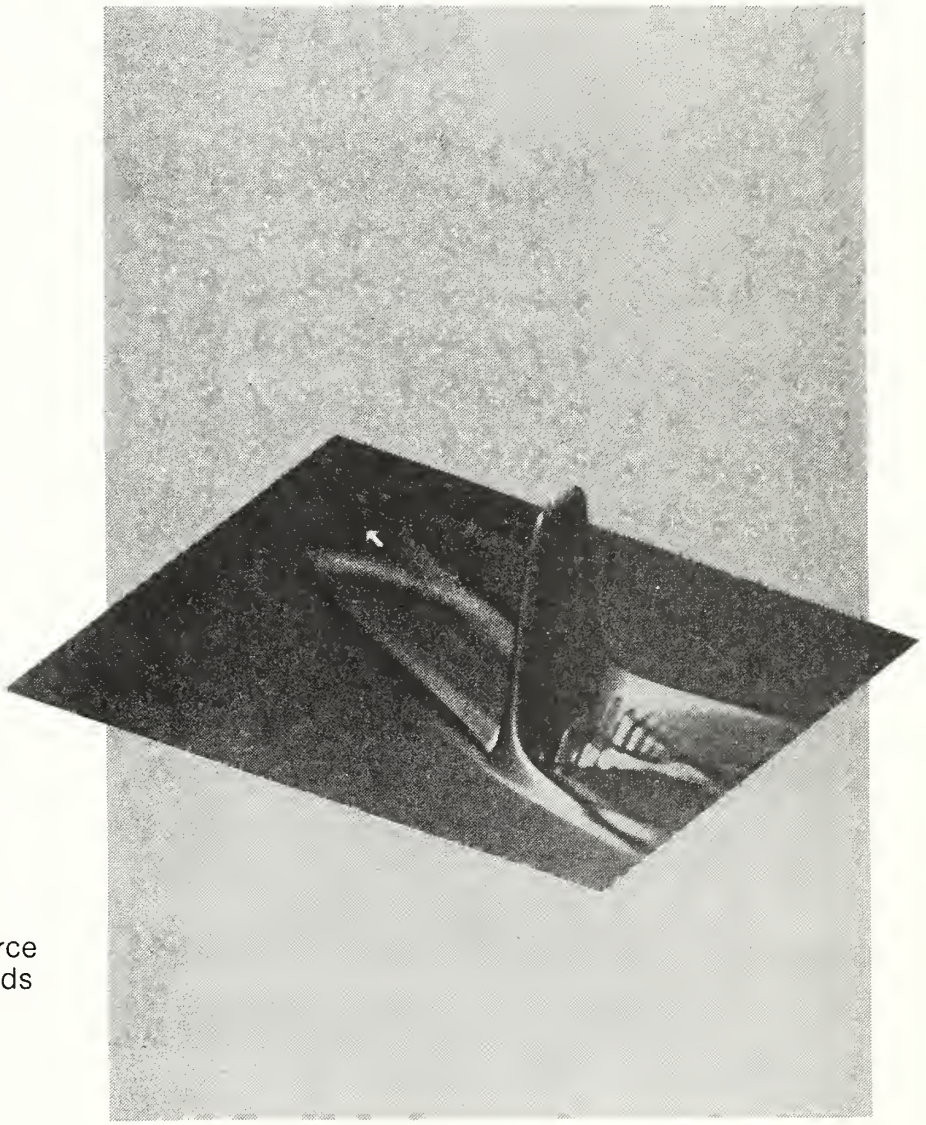

NAS-NRC
Assessment Panel
February 1–2, 1990

NISTIR 89-4149
U.S. Department of Commerce
National Institute of Standards
and Technology

Technical Activities 1989

This figure shows a stress wave simulation (and visualization) of a single quasitransverse (QT) wave propagating in an off-axis unidirectional graphite/epoxy composite where the quasilongitudinal (QL) wave has been eliminated (see white arrow) by preferentially launching the QT wave with the eigenvector solution to Christofell's equations. With only the QT wave present, the shift in propagation direction of the QT wave used in patent no. 4,499,770 can be made much more accurately with a linear array of acoustic transducers at the far boundary. This simulation on the NIST supercomputer and visualization by collaboration with Precision Visuals, Inc. has aided NDE designers in understanding and improving an existing NDE technique.

IMSE

Institute for Materials Science and Engineering

FRACTURE AND DEFORMATION

H. I. McHenry, Chief
C. M. Fortunko, Deputy Chief

NAS-NRC
Assessment Panel
February 1-2, 1990

December 1989

NISTIR 89-4149
U.S. Department of Commerce
National Institute of Standards
and Technology

Technical Activities 1989

DIVISION ORGANIZATION

Harry I. McHenry, Chief
(303) 497-3268

Christopher M. Fortunko
Deputy Division Chief
(303) 497-3062

PERFORMANCE	
Fracture Mechanics	David T. Read (303) 497-3853
Fracture Physics	Ing-Hour Lin (303) 497-5791
Nondestructive Evaluation	Alfred V. Clark, Jr. (303) 497-3159
Composites	Ronald D. Kriz (303) 497-3547
PROPERTIES	
Cryogenic Materials	Richard P. Reed (303) 497-3870
Physical Properties	Hassel Ledbetter (303) 497-3443
PROCESSING	
Welding	Thomas A. Siewert (303) 497-3523
Thermomechanical Processing	Yi-Wen Cheng (303) 497-5545
ADMINISTRATIVE SUPPORT	
Administrative Officer	Kathy S. Sherlock (303) 497-3288
Division Secretary	Heidi M. Quartemont (303) 497-3251
Group Secretaries	Vonna J. Edgins (303) 497-5338 Rebecca M. Wait (303) 497-3290

INTRODUCTION

MATERIALS RELIABILITY DIVISION

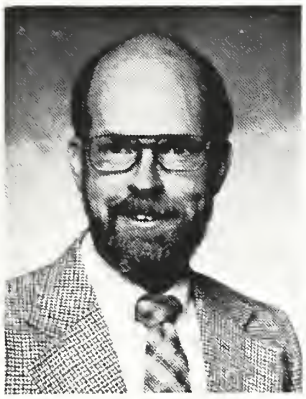

Harry I. McHenry
Chief

Christopher M. Fortunko
Deputy Chief

The Materials Reliability Division, formerly the Fracture and Deformation Division, conducts materials research to improve the quality, reliability, and safety of industrial products and the nation's infrastructure. Our research fosters the use of advanced materials in commercial products by improving confidence in their service performance. We do this by developing measurement technology for:

1. process control which improves the quality, consistency and producibility of materials

2. nondestructive evaluation (NDE) which assures the quality of finished materials and products

3. fitness-for-purpose standards which relate material quality to reliability and safety

4. materials evaluation for severe applications, particularly for service at cryogenic temperatures.

Our interdisciplinary staff is organized into specific research groups in the general areas of materials performance, properties, and processing. Each group is headed by a recognized expert in that technology who provides a focal point for industrial cooperations, scientific interactions, and technology transfer.

This year, we changed our name to Materials Reliability because the new name describes our research goals and better reflects the NIST mission: "to assist industry in the development of technology and procedures needed to improve quality, to modernize manufacturing processes, to ensure product reliability ... based on new scientific discoveries." In support of the long-range plan of the Materials Science and Engineering Laboratory, our new programs focus on advanced materials with high commercial

potential and on automated processing, which is the key to improved productivity in the materials industry. We also conduct materials research for other government agencies and provide technical services to industries, universities, and other scientific laboratories.

American industry leads the world in the development of advanced materials, but frequently we trail in using these materials for commercial products. The commercial lag is due to lack of confidence in the service performance of advanced materials, particularly safety and reliability. The Materials Reliability Division programs are developing measurement methods, sensors, standards, and reference data that will be used to measure the quality of advanced materials and to assess their service performance. Once measurement methods and standards are developed, industry can confidently use advanced materials to design and manufacture new products.

RESEARCH STAFF

Austin, Mark W.	• Radioscopy • Elastic properties • X-ray diffraction
Berger, J. R.	• Fracture mechanics • Photomechanics • Dynamic fracture
Cheng, Yi-Wen	• Fatigue of metals • Thermomechanical processing of steels • Ferrous metallurgy
Clark, Alfred V., Jr.	• Ultrasonic NDE • Engineering mechanics • Nondestructive evaluation
Fitting, Dale W.	• Sensor arrays for NDE • Ultrasonic and radiographic NDE • NDE of composites
Fortunko, Christopher M.	• Ultrasonic transducers and instrumentation • Nondestructive evaluation • Analog measurements
Kim, Sudook	• Elastic properties • Low-temperature physical properties • Ultrasonics
Kriz, Ronald D.	• Finite-element analysis for composites • Mechanics of composite materials • NDE of composite materials
Ledbetter, Hassel M.	• Physical properties of solids • Theory and measurement of elastic constants • Martensite-transformation theory
Lin, Ing-Hour	• Electronic materials • Physics of fracture • Dislocation theory
McCowan, Chris N.	• Welding metallurgy • Mechanical properties at low temperatures • Metallography and fractography
McHenry, Harry I.	• Fracture mechanics • Low-temperature materials • Fracture control

Purtscher, Pat T.	• Fracture properties of metals • Metallography and fractography • Mechanical properties at low temperatures
Read, David T.	• Electronic packaging • Elastic–plastic fracture mechanics • Mechanical properties of metals
Reed, Richard P.	• Mechanical properties • Low-temperature materials • Martensitic transformations
Schramm, Raymond E.	• Ultrasonic NDE of welds • Ultrasonic measurement of residual stress • Electromagnetic acoustic transducers
Shepherd, Dominique	• Charpy impact testing • Metallography and fractography • Thermomechanical processing
Shull, Peter J.	• Capacitive-array and eddy-current sensors • Electronics for EMATs • Nondestructive evaluation
Siewert, Thomas A.	• Welding metallurgy of steel • Gas–metal interactions during welding • Welding database management
Simon, Nancy J.	• Material properties at low temperatures • Database management of material properties • Handbook of material properties
Tobler, Ralph L.	• Fracture mechanics • Material properties at low temperatures • Low-temperature test standards
Walsh, Robert P.	• Mechanical properties at low temperatures • Mechanical test equipment • Large scale testing
Yukawa, Sumio	• Fracture mechanics • Codes and standards • Structural safety

TECHNICAL ACTIVITIES

PERFORMANCE

The Nondestructive Evaluation, Composite Materials, Fracture Mechanics and Fracture Physics Groups work together to detect damage in metals and composite materials and to assess the significance of the damage with respect to service performance.

Nondestructive Evaluation

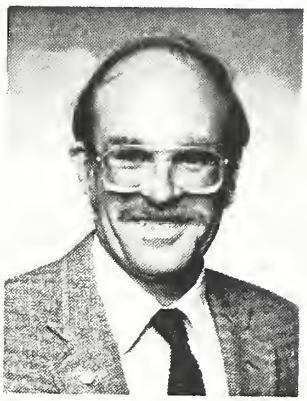

Alfred V. Clark, Jr.
Group Leader

D. W. Fitting, D. V. Mitraković,* R. E. Schramm, P. J. Shull

Our Nondestructive Evaluation (NDE) group develops measurement methods and sensors for evaluating the properties and the processing of materials. To improve structural safety, we use electromagnetic acoustic transducers (EMATs) to detect and size flaws and to measure residual stresses. For advanced materials, we develop sensors to monitor elastic property degradation in polymeric composites, sintering of ceramics, curing of polymers, and crystalline texture in steel sheet.

Representative accomplishments

- A prototype EMAT-based formability sensor was developed for evaluation by the industry.
- A prototype EMAT-based inspection system was developed to detect flaws in railroad wheels.
- A linear acoustic array was developed to inspect composite materials.

Technical Highlights

Ultrasonic Techniques

The NDE Group is developing three ultrasonic instrumentation systems for flaw detection and materials characterization. Two of these systems use noncontacting electromagnetic acoustic transducers (EMATs), and the third uses an array of piezoelectric polymeric transducers made of polyvinylidene fluoride (PVDF). Both of the EMAT-based systems were designed as prototype

---

*Guest worker from the University of Belgrade, Belgrade, Yugoslavia.

instruments that will be delivered to the sponsor for on-site evaluation. We believe that delivery of a working prototype system to a sponsoring agency or industrial entity is an essential part of the technology-transfer process.

One of the EMAT-based systems is intended for use at a stamping plant where it will be used to determine the formability index $\bar{r}$ of sheet steel. The other will be delivered to the American Association of Railroads, which will evaluate it at its facility in Pueblo, Colorado. In both cases, NIST will assist in carrying out the field evaluations.

Formability Index Determination

The concept of the EMAT-based system for formability determination is depicted in block diagram form in Figure 1. A high-current amplifier drives the transmitting EMAT, which generates a guided mode in the plane of a thin steel sheet. The wave is detected by the receiving EMAT, is amplified, and becomes as input to a digital gate. When a selected zero crossing in the waveform occurs, the gate sends a signal to stop a time-interval-averaging counter. The counter has meanwhile been running, having been started by a signal synchronous with the pulsing of the current amplifier.

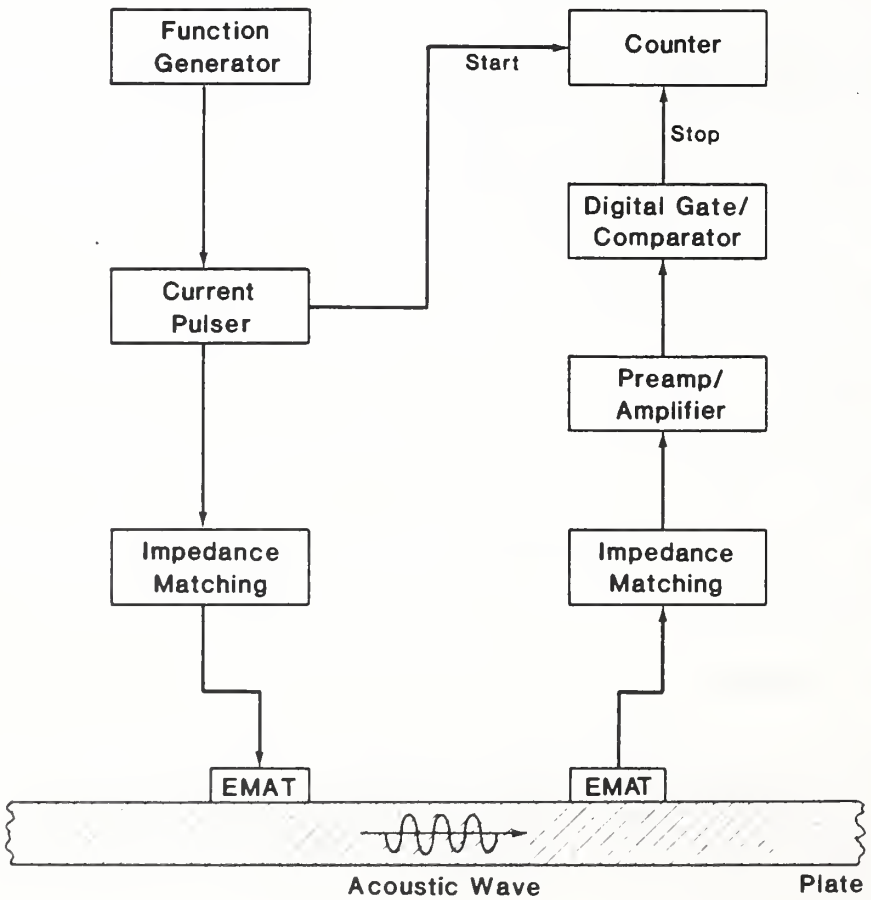

Figure 1. The ultrasonic system for measuring the formability of steel sheet.

The electronics have been developed at NIST in collaboration with Professor D. V. Mitrakovic' of the University of Belgrade. Careful attention has been paid to grounding and shielding to maximize the signal/noise (S/N) ratio of the system. In thin steel sheet, a typical S/N can be as large as 100:1 with the EMATs in close proximity to the sheet.

The system is used to measure the velocity of guided waves propagating at different directions to the sheet rolling direction. It is known from first principles that the average of velocities, $\bar{V}$, of waves propagating at 0^0, $\pm 45^0$, and 90^0 to the rolling direction will be related to the formability of the thin steel sheet.

In industrial practice, formability is typically measured by cutting unidirectional tensile samples from the ends of coils of sheet. The samples are plastically deformed, and the strain ϵ_w and ϵ_t in the sample width and thickness direction are measured. The r-value is the ratio: $r = \epsilon_w/\epsilon_t$. The r-value is measured for specimens at 0^0, 45^0, and 90^0 to the rolling direction.

The average r-value, $\bar{r}$, is a commonly used measure of sheet formability, where $\bar{r} = [r(0^0) + 2r(45^0) + r(90^0)]/4$. From theory, it is known that V and $\bar{r}$ should be related.

Researchers at NIST have been collaborating with colleagues at Iowa State University and Osaka University (Japan). Specimens of rolled steel sheet have been obtained from Ford Motor Company and Sumitomo Metal Industries (Japan). The companies measured the r-values for these specimens using destructive techniques.

Several of the specimens were sent to each laboratory (NIST, Iowa State, Osaka University) to cross-check the ultrasonic measurements. These measurements were found to be in good agreement with each other.

Some of the steel sheets were coated for corrosion resistance. A simple correction of the effective mass and stiffness of the coating was developed by Osaka University. This caused a small correction to be made to the ultrasonic velocities. When this correction is made, the correlation between $\bar{r}$ and $\bar{V}$ is as shown in Figure 2.

This excellent correlation indicates that the ultrasonic system could be used to accurately characterize the formability of thin steel sheet. One possible application is in a stamping plant, where pieces of sheet metal are formed into automobile body parts.

Recently, a collaboration has been initiated between NIST and an automotive company. The goal of this collaboration is to transfer NIST technology to a stamping plant. To this end, a fixture has been designed and built by the company to house and rotate the transmitting and receiving EMATs. The EMATs and a portable rack of electronics have been constructed at NIST. The electronics are "user-friendly" and will require no adjustments once delivered to the company. Considerable care has been taken to harden the

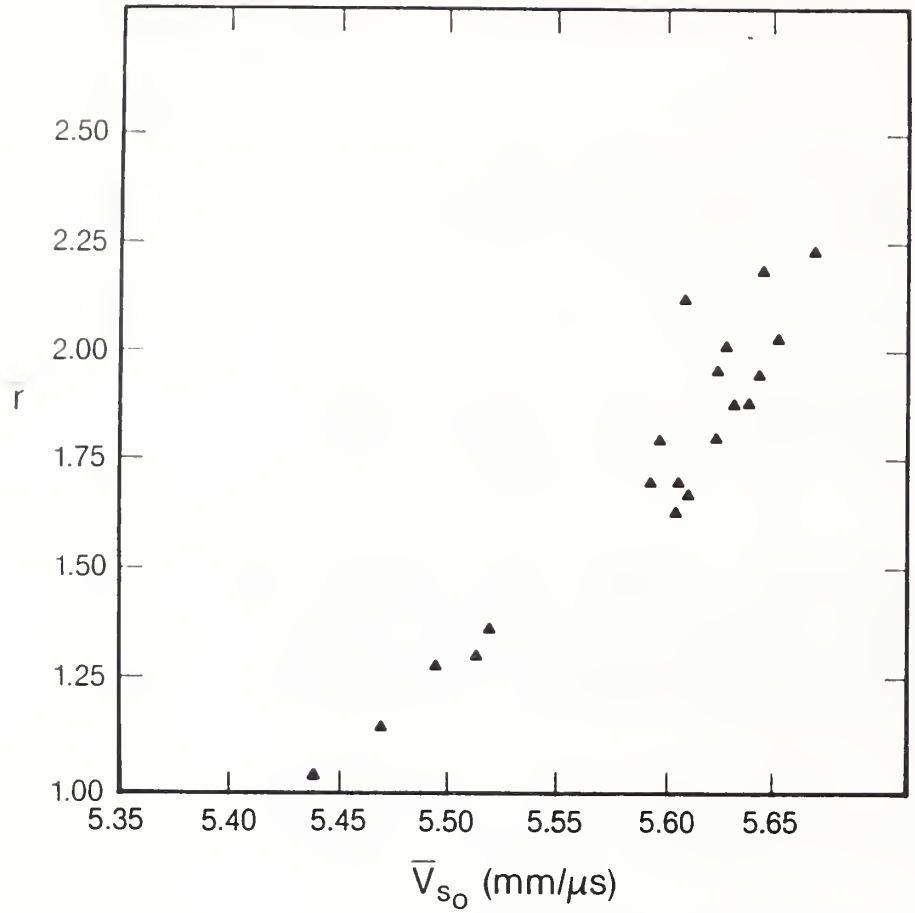

Figure 2. The correlation between the formability index, $\bar{r}$, and the average ultrasonic velocity $\bar{V}$ for steel sheets.

electronics for use in an industrial environment. Upon completion of testing, the system (fixture, EMATs and electronics) will be delivered to the company for evaluation in the quality assurance department of a stamping plant.

EMAT-Based System for the Federal Railroad Administration

In FY 1989, we also developed a prototype EMAT-based system for detecting flaws in railroad wheels. This system was developed under contract to the Federal Railroad Administration (FRA). In this system, an EMAT package will be placed in a cavity cut into the head of a rail. As a railroad wheel rolls over the EMAT package, surface waves in the tread of the wheel will be generated by a transmitting EMAT. Echoes caused by surface cracks will be detected by a receiving EMAT. A signal processing algorithm will be used to determine whether the crack is above or below a critical size.

An exploded view of the EMAT package is shown in Figure 3. The package contains the two EMATs, which generate and receive the surface waves. The compliant backing assures that the EMAT coils will conform closely to the profile of the tread; this is necessary to ensure a good coupling of ultrasound from the EMAT into the wheel. Also in the package are two switches, which activate a trigger circuit. This circuit in turn causes a high-current amplifier to pulse the transmitting EMAT.

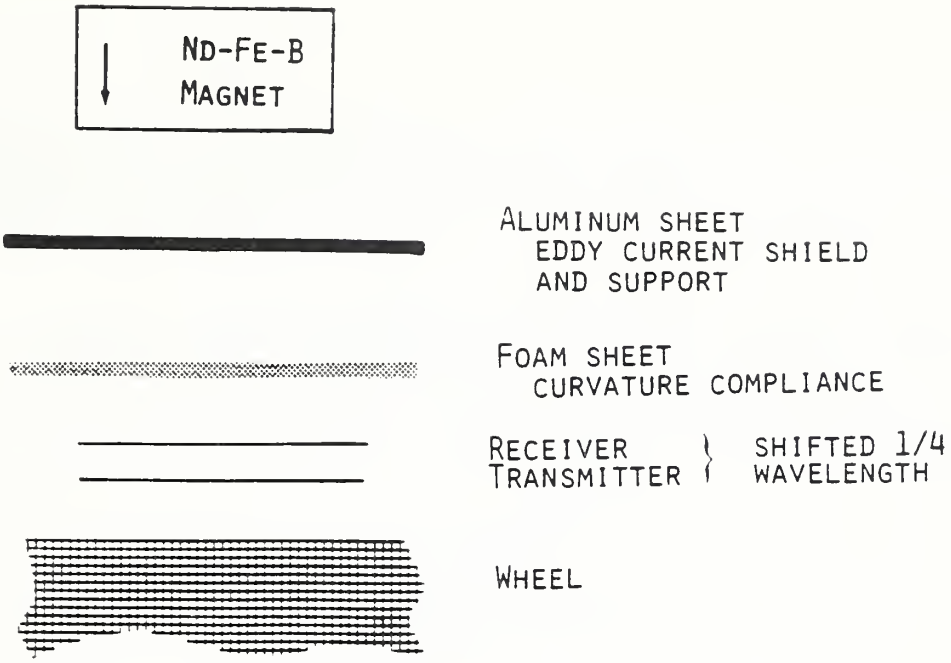

Figure 3. The EMAT package used to inspect railroad wheels.

The amplifier has been hardened in anticipation of field tests at the Transportation Test Center (TTC), operated for the FRA by the American Association of Railroads (AAR). A low-noise, high gain voltage amplifier has also been developed in order to amplify the signal detected by the receiving EMAT. This amplifier has also been hardened.

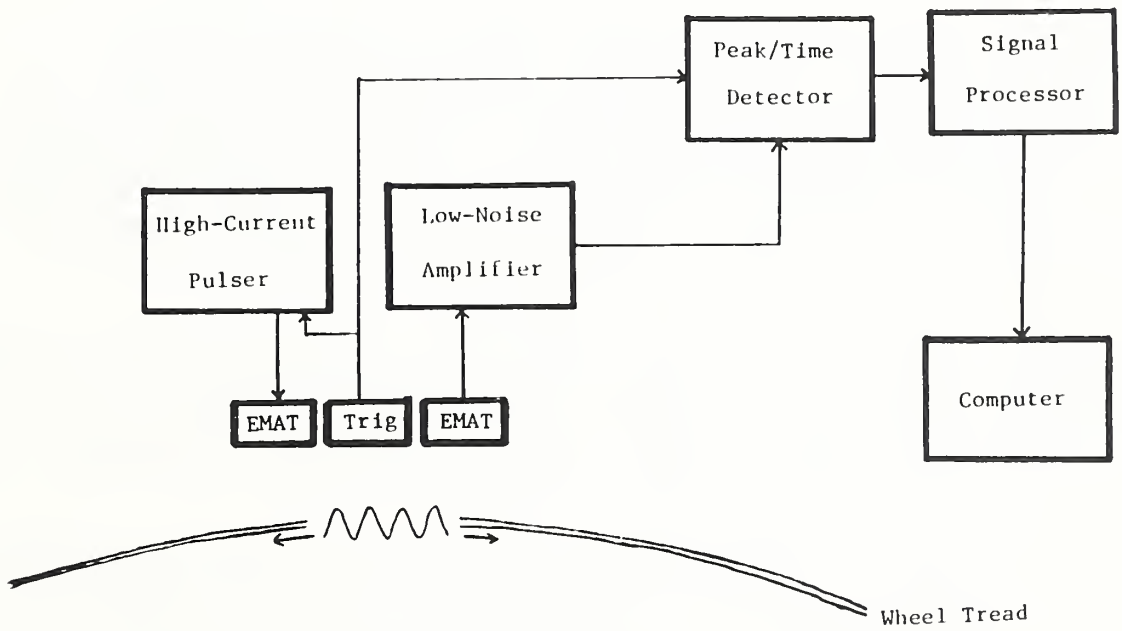

Figure 4. Schematic of the ultrasonic measurement system used to inspect railroad wheels.

Tests have recently begun on a hybrid analog/digital system which operates on the signal from the voltage amplifier (see block diagrams in Figure 4). This system was developed as part of a collaboration between NIST and the University of Belgrade.

The hybrid system detects peaks in the received waveforms, and the corresponding times at which they occur. The data become the input to a microcontroller. This device implements an algorithm which: a) compensates for the attenuation as the wave transits the wheel; b) compensates for the degree to which ultrasound is coupled from the EMAT into the wheel; c) takes the compensated values and predicts whether the defect size is critical or noncritical.

The results of the signal processing algorithm are stored in a data-logging computer. A separate computer (not shown for simplicity in the block diagram) also records a digitized version of the analog waveform. This will allow debugging of the hybrid system, by recording the actual input into that system and comparing the input with the output of the microcontroller.

Initial tests have begun to test the entire system starting from trigger to analog electronics to hybrid system to computer. These tests have been done by manually rolling a wheel with a known defect over the EMATs. Upon successful completion of these laboratory tests, the system will be taken to the TTC for field tests. In these tests, actual rolling stock (freight cars) will be pulled behind a locomotive. The reliability of the system will be checked as a function of train speed, size of defect, and degree of tread wear.

Ultrasonic Arrays for Characterization of Polymer-Matrix Composites

We have continued development of ultrasonic transducer arrays for characterization of composite materials. In FY 1989, new arrays have been fabricated with elements which are less responsive to acoustic interference. Measurements were made with these arrays on samples of composite panels. Algorithms have been developed to recover ultrasonic properties of the specimen which relate to their elastic moduli.

Several measurement configurations using our arrays have been explored. For each configuration, algorithms were developed to recover the group velocity and energy flux angle of bulk waves as well as the phase velocity and direction of the wavefront normal. These intrinsic quantities can be determined from the spatial location of the center of the received beam and the arrival time of the wavefront at the array.

Transmission-mode measurements were made with pairs of complementary wedges Figure 5. The transmitting wedge was used to direct the beam into the composite at the desired angle. A second wedge, with the same angle, was placed on the opposite side of the composite. Quasilongitudinal and quasi-transverse waves propagating in the composite convert at this second wedge

boundary into bulk modes which arrive at normal incidence upon the array. The center of the wavefield arriving at the array for this measurement configuration is simply at the element which the wavefield first arrives.

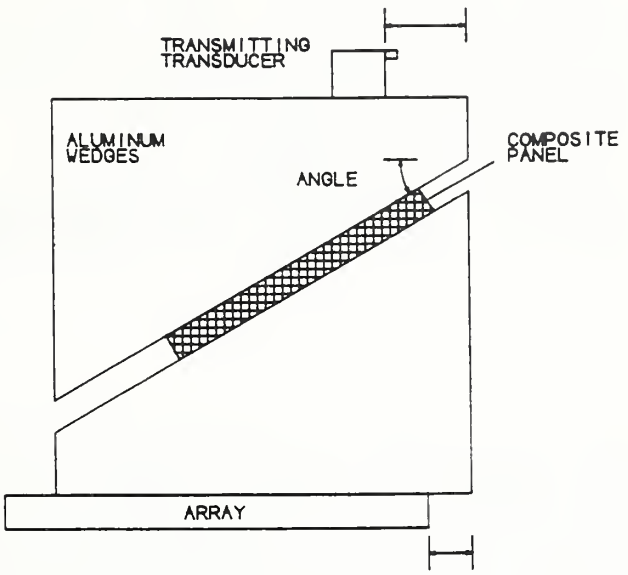

Figure 5. The paired wedge technique for making measurements on a composite yield a wave incident normally on the receiving array

An algorithm was developed for processing the array data sets, Figure 6a, generated with the dual wedge technique. The spatial location of reverberation echoes and the echo separation time are used to calculate the ultrasonic parameters relating to elastic moduli of the composite. A cross-correlation technique was used to automate wavefront mapping, Figure 6b, from which the beam center and arrival time could be extracted.

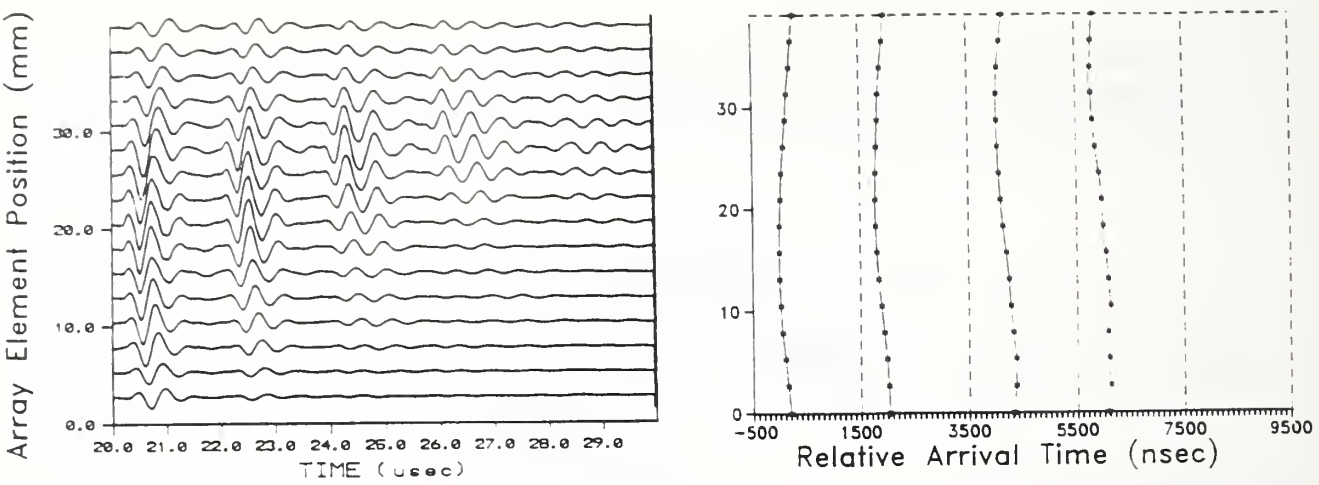

Figure 6. Array Data Set (a) for a composite plate obtained with the two-wedge, reverberation-echo technique. Note that the reverberation echoes are separated both spatially and temporally. (b)-Cross-correlation processing of the array data set provides information on location of the wavefront center and the time separation of reverberation echoes.

Electromagnetic Techniques

Capacitive-Probe Development

The NDE Group is also contributing to NIST's activities in electromagnetic characterization of materials. Capacitive array probes are used in research aimed at improving the quality of ceramics. Because these materials are nonconducting, their dielectric constants may provide information about processing parameters such as void content, densification, and degree of sintering.

The basic concept is illustrated in Figure 7. An array of electrodes lies in a plane at distance, d, above a medium with dielectric constant, ϵ. To measure the capacitance, the current, i, that flows into the receiver electrodes is measured and the capacitance calculated from $|C| = i/\omega\bar{V}$ where ω = frequency of the voltage source, $\bar{V}$.

The probe can operate in either of two modes: contacting, or noncontacting. In the former case, d = o; in the latter, d, is unknown in general. For certain materials (such as superconducting ceramics), it is necessary to operate in the noncontact mode to avoid contamination problems.

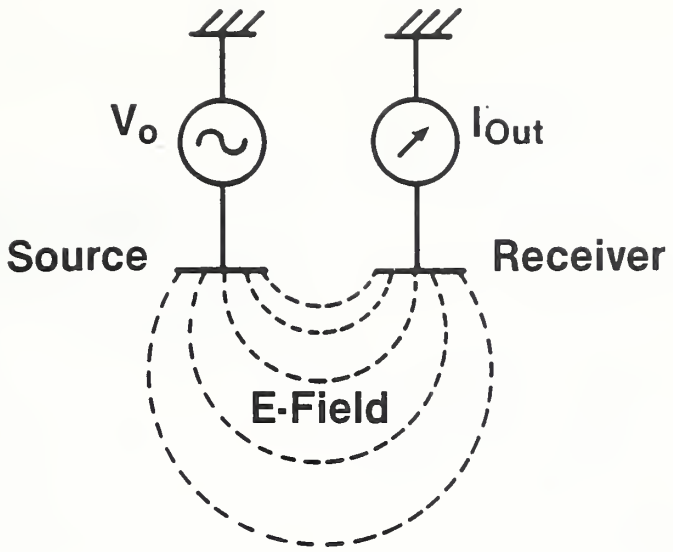

Figure 7. The basic concept of the capacitive probe.

One possible way to determine ϵ when d is unknown is to vary the pattern of potential impressed on the probe electrodes. This changes the shape of the electric field, and thus changes the probe's response to the dielectric material. In principle, we could vary the potential pattern, measure the resulting capacitance, and use an inversion algorithm based on theory to obtain ϵ.

An elementary theory (developed by Prof. B. A. Auld at Stanford University) predicts an almost exponential decrease of probe capacitance with increasing d (liftoff). The theory assumes that the probe field does not interact with any conductors in the vicinity of the dielectric. This interaction can occur, for example, if there is an average voltage on the probe electrodes. If this occurs, then the probe effectively becomes one plate of a capacitor, and any other conductors in the environment become the other plate. In this configuration, the total current into the electrodes will no longer decrease monotonically with liftoff.

New electronics have been constructed which appear to give a balanced voltage on the electrodes (average voltage = 0). A block diagram of the system is shown in Figure 8. A balanced voltage source, which does not have one side tied to ground, impresses a potential across a reference capacitor, C_{Ref}, and the probe electrodes, C_p. The current flowing through the precision resistors is measured with high input impedance differential amplifiers. The difference in voltage, $V_p - V_{Ref}$, is proportional to the difference in capacitance, $C_p - C_{Ref}$. The voltage difference is measured with another differential amplifier (not shown). In practice, C_{Ref} is trimmed to be approximately equal to C_p, to avoid dynamic range problems.

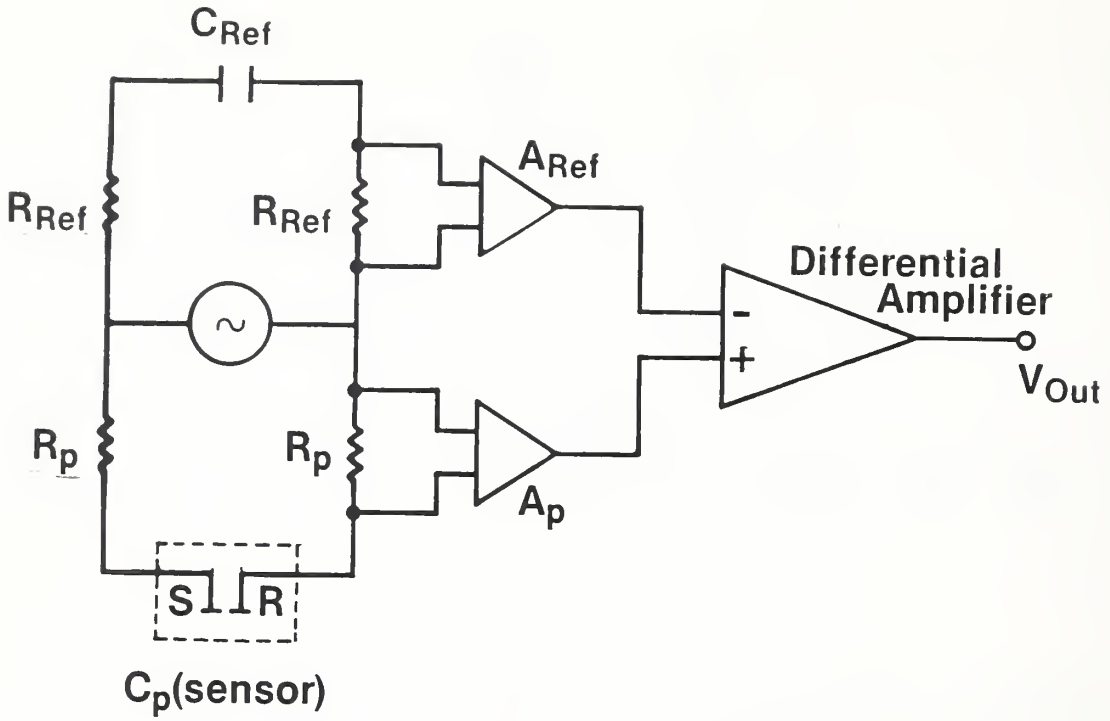

Figure 8. Schematic of the capacitance measurement system.

It is crucial to keep the impedance of the amplifier large relative to the impedance of the capacitors; otherwise the current will simply be shunted through the amplifiers and all sensitivity to change C_p-C_{Ref} will be lost.

The circuit has been tested on several ceramic specimens. A typical result is shown in Figure 9 where the probe admittance change, ΔY, is plotted as a function of liftoff. The magnitude of probe admittance, $|Y|$, equals ωCs. Also plotted is the prediction of the elementary theory, which is forced to fit the experiment at the data point having the smallest liftoff. Reasonably good agreement is obtained with the elementary theory.

For high dielectric materials, a different approach is necessary. For most values of d, the electric field cannot penetrate the surface of the dielectric, due to the high polarizability of the material at the surface. The electric field lines are "bent" as they reach the surface and effectively "skim" the surface. This causes loss of probe sensitivity to the material's dielectric properties.

An exception occurs for small d. Here, the probe field is locally normal to the surface, and can be forced into the dielectric. However, in this regime, some of the assumptions of the elementary theory are no longer valid, and a new approach is necessary.

A new theory has recently been developed in collaboration with Dr. V. Tewary. The theory gives the exact solution of the electric field in all space, including the immediate vicinity of the electrodes (where the elementary theory breaks down).

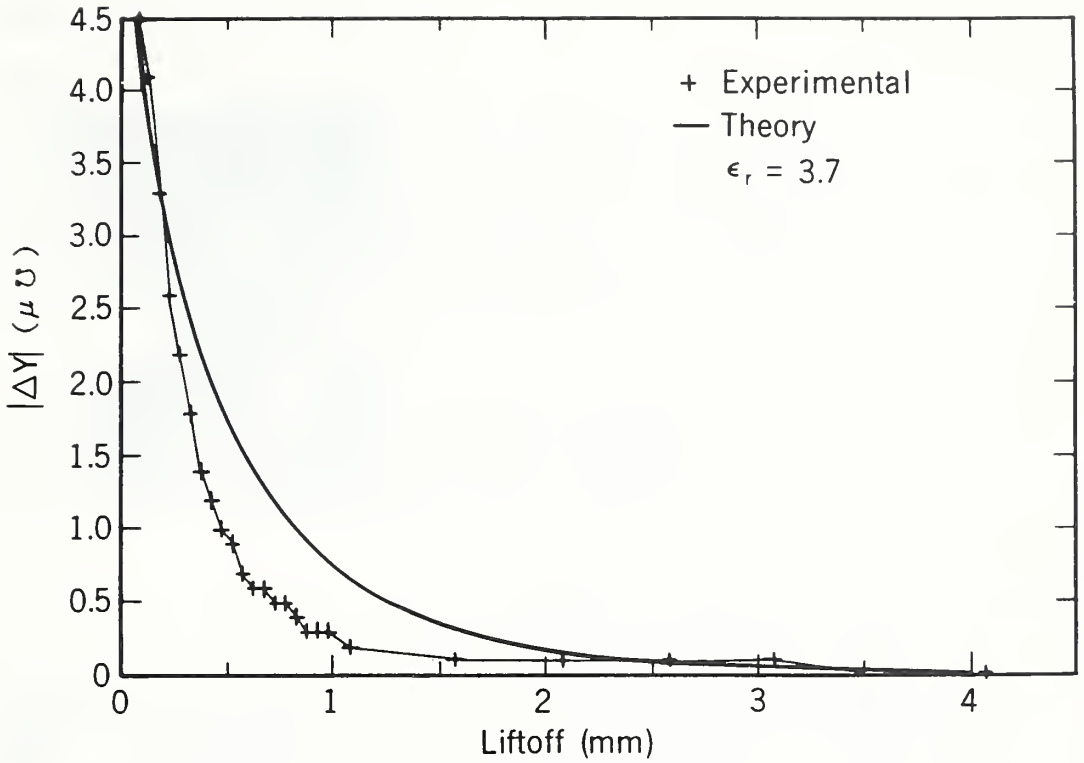

Figure 9. A comparison of measurements of probe admittance change, ΔY, as a function of liftoff with the theoretical predictions of Auld.

Experiments will be performed to verify the predictions of this theory. Then an inversion algorithm will be developed to obtain the dielectric constant from capacitance measurements.

Composites

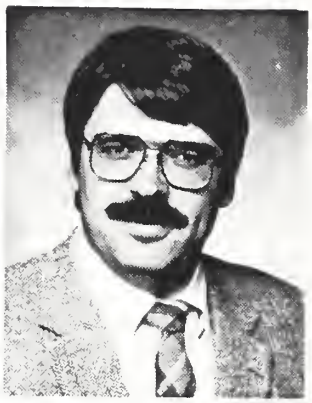

Ronald D. Kriz
Research Leader

J. R. Berger, J. D. McColskey, V. Tewary*

Our research in composite mechanics emphasizes (a) the mechanics of fracture and (b) the mechanics of nondestructive evaluation of fiber-reinforced composite materials. Our approach is analytical and experimental. Unlike metals that are typically homogeneous and isotropic, fiber-reinforced composites can be designed for specific applications by controlling their wide range of parameters, which include fiber volume fraction, fiber orientation, interface properties, laminate stacking sequence, and fiber-matrix elastic properties. We study how these design parameters relate to the mechanical performance of selected composites.

Representative accomplishments

- Laminate Interface Singularities - Interface singularities have been obtained for the generalized-plane-strain "free-edge" laminate problem. These singular fields where the bimaterial interface terminates at the stress free edge includes the lm(r) singularity predicted by Ting (1989) using Stroh's method. With the correct Green's function, a variety of interface problems related to laminate damage studies can be studied.

- Numerical Simulation and Visualization of Stress Wave Propagation in Graphite/Epoxy Composites - The purpose of the simulation was to aid the nondestructive evaluation engineer in designing an acoustic array to improve the measurement of the shift in the QT wave propagation direction (Patent No. 4,499,770). In this study, we demonstrated the advantage of using a finite difference model to simulate this experiment and with special visual aids observe the physics and recommend improvements in the patent measurement.

---

*Visiting scientist from Ohio State University, Columbus, Ohio.

Composite fracture mechanics

Fracture mechanics is not as well established for composites as it is for homogeneous, isotropic materials because each laminated composite has its own types and sequence of damage mechanisms. Therefore, we have been developing new analytical and experimental methods to understand the physical significance of different kinds of damage in laminated composites (ply cracks, interface cracks, delaminations, edge stresses). For sponsors, we have measured the mechanical properties of new materials that are candidates for specific applications.

A. Analytical method for calculating singularities in laminates

As part of a long-term project, we are studying a Green's function approach to predict a near field singularity at several types of bimaterial interfaces, Figure 10, that exist in laminated structural composites.

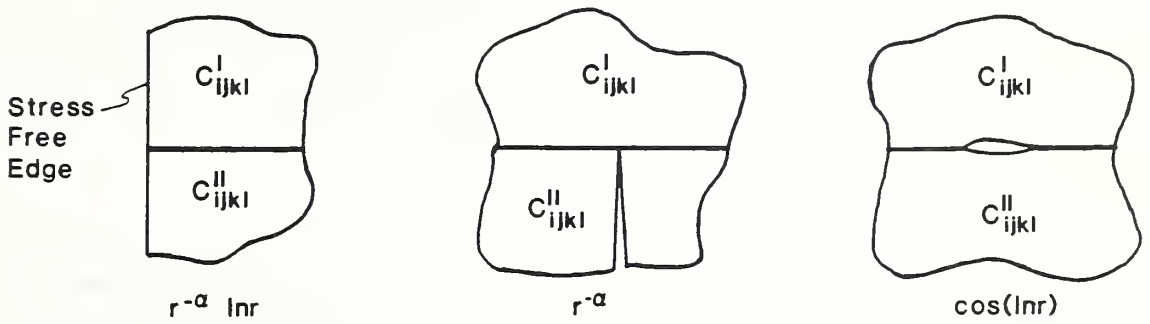

(a) free edge (b) ply crack (c) delamination

Figure 10. Types of singularities at anisotropic bimaterial interfaces.

Green's function singular fields have already been published for delaminations by Tewary, Hirth, and Wagner. Recently, we have solved the generalized-plane-strain, free-edge laminate problem with a Green's function. In Figure 11, we show a distribution of the "peeling" stress along the bimaterial interface near the free edge which must be continuous across the interface but singular at the free edge.

Studies include several laminate configurations ($\pm\theta$ symmetric stacking sequences and cross ply 0/90). Combinations of these configurations will be studied using enriched finite elements to include the near field singularities in the total boundary-value problem which is solved numerically. Previous studies have used a numerical approach which cannot properly model the singularity. An analytic singular solution can model the singularity accurately but because of the analytic complexity, this approach can be used for only a few special boundary conditions. Obviously, a complete analytic model of the singularities, geometries, and boundary conditions of multilayer laminates would be extremely difficult

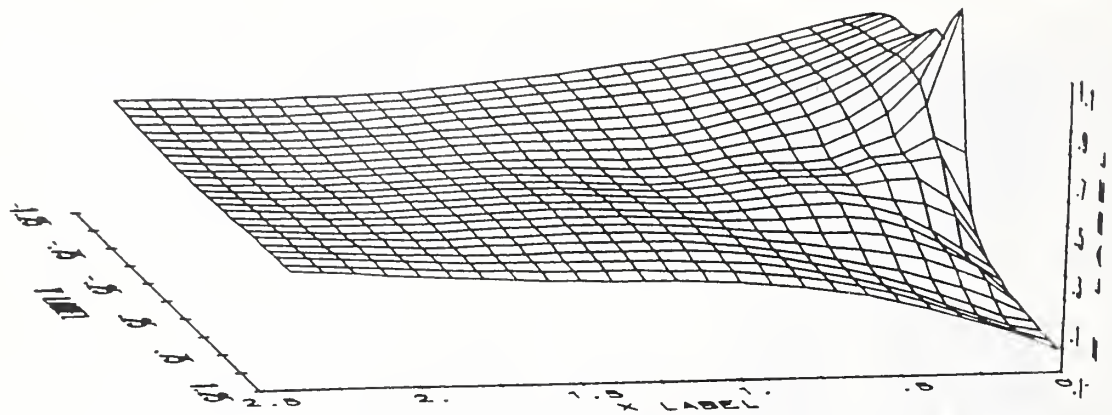

Figure 11. Stress normal to bimaterial interface separating two anisotropic regions

if not impossible. For these damaged structural laminates, a hybridized analytic-numeric model is required.

B. New composite materials for thermal-isolation straps

A new Al_2O_3 (alumina) fiber composite with high strain to failure was fabricated with a thermal plastic PEEK (poly-ether-ether-ketone). The Al_2O_3-PEEK composite shows a marked improvement over thermally setting composite in that it absorbs 150 percent more elastic strain energy at 76 K than at room temperature (Figure 12). This increases in fracture toughness at low temperatures can provide improved fatigue performance for thermal isolation straps at low temperature. Other mechanical property results suggest improvements for applications where graphite-epoxy materials are presently being used at low temperatures and where light weight is not a critical issue.

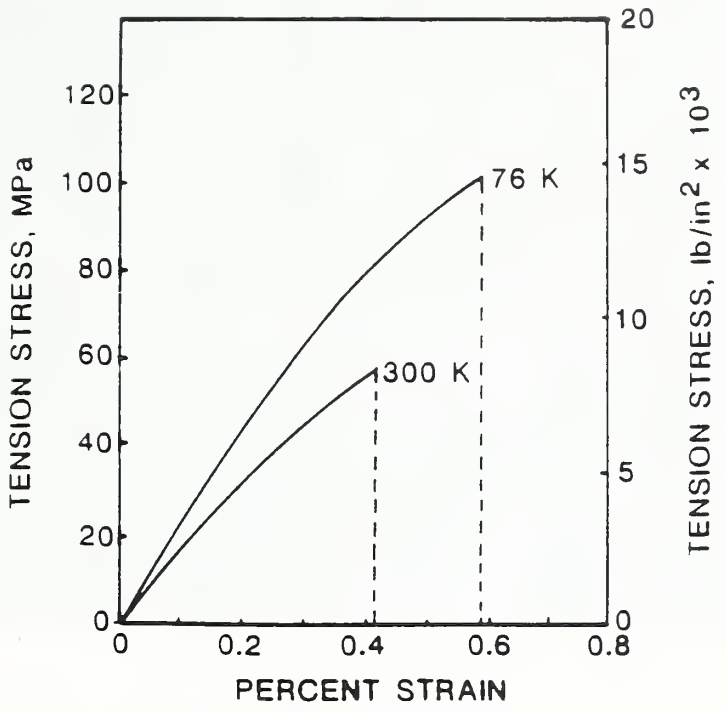

Figure 12. Stress-strain curve of $[90_{16}]$ Al_2O_3/PEEK.

Mechanics of nondestructive evaluation for composites

Our nondestructive evaluation (NDE) studies concentrate on (a) measuring and mapping the mechanical deformation near damage in a composite laminate with optical diffraction techniques and (b) developing a numerical model to predict the full-field deformation topologies of stress waves propagating through an off-axis unidirectional graphite/epoxy composite. Both efforts emphasize modeling the *mechanics* of deformation as it relates to damage in a quasi-static state of deformation or as it relates to the dynamic deformation of a propagating stress wave.

A. Determination of strain fields in damaged composite panels

Because damage in composite structural laminates is heterogeneous, an inhomogeneous distribution of strains corresponds to the growth of this damage. To map the distribution of this heterogeneous strain field, an optical strain-measurement technique has been developed which is fully automated. Several improvements have been realized on the NIST Optical Diffraction Strain Measurement System (ODSMS) which were described in previous annual reports (1987 and 1988). Briefly, the ODSMS uses the optical diffraction of a coherent light source to measure localized strain

over a portion (1-mm diameter) of a deformed moiré grid, which is attached to the surface of a specimen while under load. Strain is calculated from changes measured in the diffraction pattern, which corresponds to in-plane deformation of the moiré grid.

A point-by-point measurement of all three in-plane components of strain can be made by observing the change in the optical diffraction pattern from a grating under deformation. As described in previous work on this particular grid method, photographic negatives are made of a specimen grating in an undeformed state and at various stages of deformation. The negatives of the diffraction grating are then interrogated separately in an automated optical post-processor.

The technique requires precise registration between the negatives for the strain analysis. In the presence of periodic or random errors in grating frequency, large apparent strains can be measured because the negatives are out of registration.

Data obtained from a 40 line/mm crossed-line grating attached to a centrally cracked aluminum panel is shown in Figure 13. This gray scale plot was generated by comparing the diffraction pattern from the undeformed grating with a hypothetical perfect grating. The apparent strain resulting from this comparison can be calculated (point wise).

The specimen grating clearly contains a large periodic error as can be seen in Figure 13. If there is any registration error when analyzing the deformed grating, an obvious apparent strain will result. The registration problem was successfully solved by both an optical technique involving fiducial marks as well as a cross-correlation performed in software. The cross-correlation procedure adequately registers the two waveforms to determine the strain along a particular section with a noise level of approximately $\pm 100\ \mu\epsilon$.

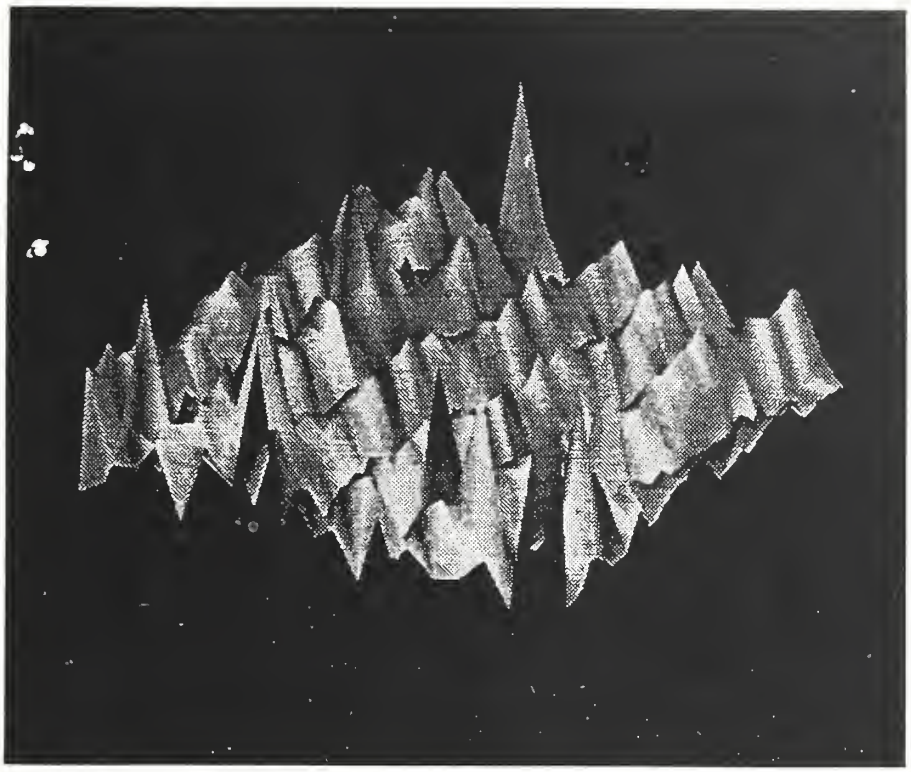

Fig. 13. Apparent strain in the undeformed grating.

B. Stress-wave topologies in off-axis graphite/epoxy composites

Within the last ten years, there has been a renewed interest in simulation of stress wave propagation by a number of investigators because of the availability of faster supercomputers with large memory capabilities. Only recently have a few investigators applied these simulations to problems where elastic anisotropy was included as a major factor in the physical problem being studied. The massive output of results from these simulations together with the added complexity of coupled phenomena that uniquely exist for a given anisotropy defies intuition and requires scientific visualization to facilitate understanding and interpretation. Often such visualizations required a movie format to better understand the physics of a particular problem. In this study, we chose to simulate the experimental measurement of a shift in the quasitransverse bulk wave propagation in an off-axis unidirectional graphite/epoxy composite in plane strain (Patent No. 4,499,770). The purpose of the simulation was to aid the nondestructive evaluation engineer in designing an acoustic array to improve the measurement of the shift in the QT wave propagation direction. Previously, a finite element model was used to simulate this measurement. This study demonstrated the advantages of using a finite difference model to simulate the experiment. Special visual aids were used to observe the physics.

In Figure 14, we show how the isolation of the QT wave can also be used to improve the measurement proposed in Patent No. 4,499,770. The slower moving QT (lower right) and the faster moving QL wave (upper left), shown in Figure 14a as a displaced out-of-plane shaded surface, were generated

simultaneously from the same unipolar pulse. Here, the objective was to simulate and measure the propagation direction of the QT wave by using a linear array of acoustic transducers on the reflecting boundary. Because the angle of propagation is measured and not simply the QT wave arrival time, it is necessary to measure the wave shape. This measurement gave peculiar multiple peaks whose physical origin was unexplained. A simulation and visualization in a movie format clearly showed that the physical origin of these multiple peaks was the generation of "wakes" from the faster moving QL wave. Preferential launching of the QT waves (see Figure 14b), with its unique eigen vector, eliminated the QL wave and its wakes which suggested that an improved QT wave propagation direction measurement was physically possible if a transducer could be designed to reproduce the eigen vector ratio of longitudinal to transverse displacements. Possibly a specially cut quartz transducer would satisfy these requirements.

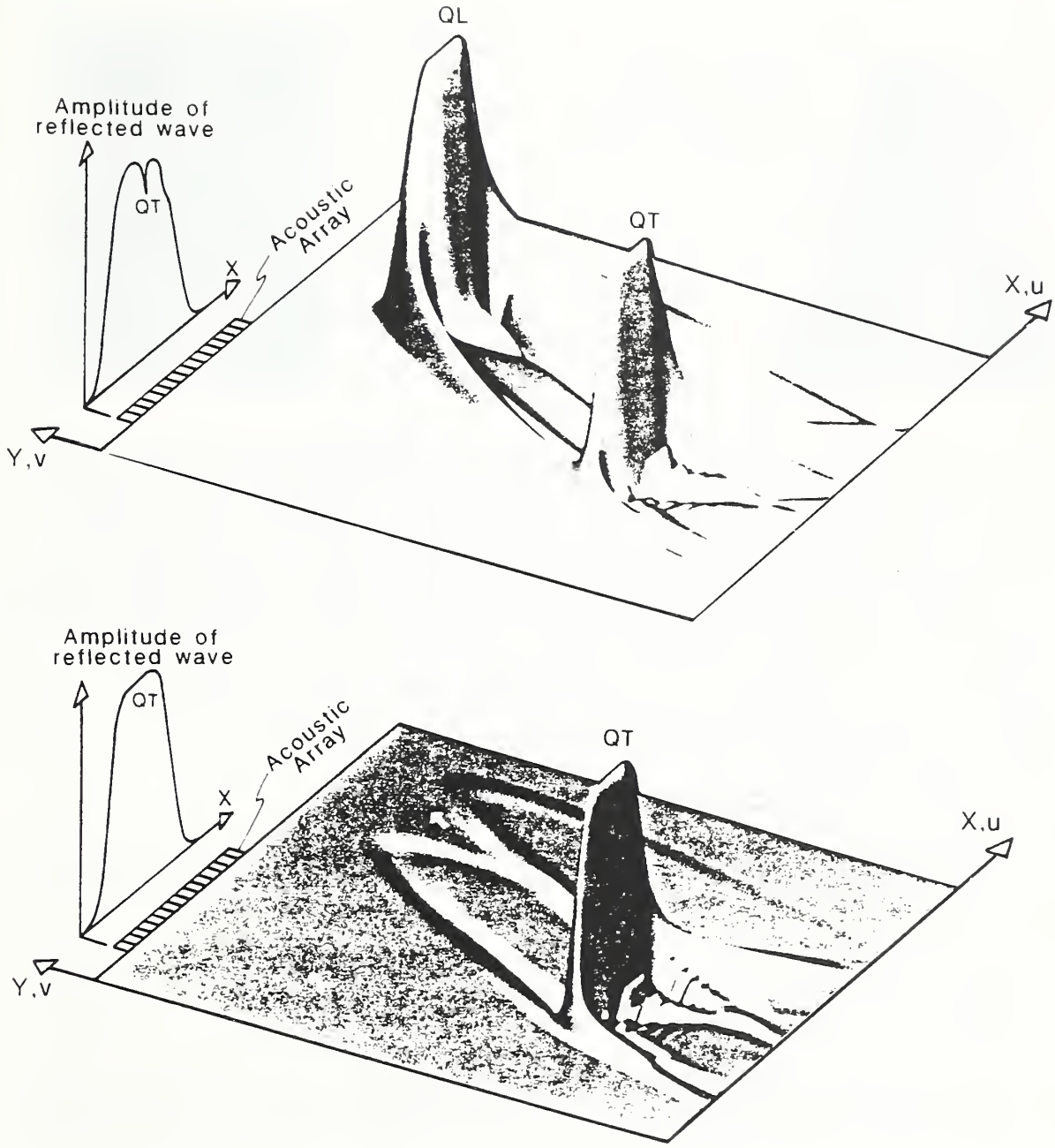

Figure 14. Isolation of the QT wave to improve amplitude measurements of the reflected wave.

Fracture

Ing-Hour Lin
Research Leader
Fracture Physics

David T. Read
Research Leader
Fracture Mechanics

Our research in the mecahnics and physics of fracture has been redirected from metals and alloys to composite materials and electronic packaging. The main shift in research has been one of scale. Traditionally, our fracture research has emphasized developing principals for using the results of small-scale experiments to predict the behavior of large-scale structures. Now, we are thinking small. In the case of composites, we are interested in damage mechanisms which are local events that deteriorate the strength and stiffness of composites, but do not necessarily trigger fracture. For electronic packaging, we are starting to develop experimental and analytical techniques for characterizing fracture behavior in thin films and multilayered materials.

Representative accomplishments

- An experimental technique was developed to detect damage in composite materials by measuring light transmittance through a multimode optical fiber during a tensile test;

- A simple model of fiber-crack interaction in composites was developed and applied to examine shielding/antishielding of fibers on the crack tip.

- Image force on dislocations and the local stress intensity for cracks along interfaces between elastically dissimilar solids were derived to study dislocation emission and interfacial failure in bimaterial solids.

- A concept for a test machine on a chip was developed which addresses an industry requirement for mechanical property data on thin films.

Composites

Damage detection using optical fibers in composites

Much research is in progress to exploit the idea of building optical fiber sensors into structural components. Useful information can be obtained during manufacture, normal use, and overstress conditions. Optical fibers can be arranged to be sensitive to a wide variety of conditions including temperature, acceleration, magnetic field, irradiation dose, pressure, and mechanical strain. In a cooperative program with an oil company, we have investigated the detection of mechanical damage using multimode fibers. The company supplied uniaxial composite rods of graphite-reinforced vinyl-ester with a multimode optical fiber embedded in the rod. We developed an experimental procedure for introducing light into one end of the specimen and detecting the transmitted light intensity at the other end while gripping the specimen for destructive mechanical testing.

The transmitted light intensity was insensitive to average axial stress or strain. The behavior in the presence of damage was interesting because it was contrary to our expectations. Instead of a complete loss of signal with the onset of damage, the transmitted light intensity decreased gradually as the damage became more severe. Only when the load-bearing capacity of the specimen rod was reduced far below its initial value did the signal vanish. We interpret this result to mean that optical fibers have the potential to give more than just a yes-or-no indication of mechanical damage. They have the potential to measure the severity of damage, and also to sense damage at multiple sites.

Fiber-crack interaction in composites

For interlaminar failure of composites, we analyzed the elastic interaction between a mode III crack, situated at the origin and a set of N line force dipoles, which physically represent rigid fibers, distributed parallel to the crack front. We considered two different fiber configurations: (1) symmetrical double-parallel layers with height, h, measured from the cleavage plane, and (2) a single perpendicular layer to the cleavage plane, with a distance, X_0, also measured from the crack tip.

Using expressions for the force and stresses derived for the line force defects, we have obtained an equation for the force on the fiber, which is important in estimating the debonding effect in composites. Also, the embrittlement toughness relation in case 1 and toughening relation for case 2 are analytically derived when the fiber spacing is much smaller than the fiber radius. We believe the local stress intensity factor at the crack tip for a precrack in a brittle polymer-matrix composite can be measured by using a photo-elastic method. To better understand the energy dissipation (or toughness) in interlaminar failure, fiber debonding and crack tip fiburcation need to be considered.

Electronic Packaging

The reliability of electronic devices is critical in many applications such

as aerospace, weapons, and certain consumer products such as safety systems in automobiles. As the performance of these devices increases, their circuit density and power consumption density also increase, leading to increased device complexity and also increased operating temperatures. Mechanical stresses arise from differences in thermal expansion coefficient among the materials which are bonded to one another to form modern electronic components and from flexure and vibration of printed circuit boards. These mechanical stresses cause cracking and fracture in brittle materials such as occur in ceramic multilayer capacitors and also result in solder joint fatigue cracking.

Fitness for service evaluation of printed circuit boards

The workhorse tool of modern advanced mechanical engineering analysis is the numerical technique of finite element analysis. Stresses are calculated based on applied loads and material stress-strain behavior. The electronics industry is beginning to apply this analysis technique both to surface mount technology (SMT) printed circuit boards (PCB) and to very- and ultra large scale integrated devices (VLSI and ULSI). We have begun programs in both areas.

For SMT PCB, we are developing a method for creating finite element meshes from X-ray laminography images of solder joints. The idea here is that solder joints are made and inspected to workmanship standards which have no solid technical basis in the relationship between the inspection criteria and the device lifetime.

Finite element analysis coupled with criteria for crack initiation, crack growth, and fracture can relate the morphology and materials of a solder joint to its fitness for service, and can predict its service lifetime and reliability. The big bottleneck is the generation of the finite element mesh, that is, a mathematical description of the device geometry which can be solved by computer to calculate stresses. These meshes were originally developed using only paper and pencil, a tedious and error-prone process.

Computer aids have advanced significantly in the last five years. We intend to take the analyst out of the loop, letting the computer modify the geometrical representation of the average solder joint for each particular case, to model the actual geometrical defects, such as insufficient or excess solder, porosity, insufficient wetting, icicles, etc., of the particular joint in question.

A concept for mechanical tests on a silicon chip

Our emphasis in the area of VLSI and ULSI devices is on the material property data needed for finite element analysis. We are developing a mechanical testing machine on a silicon chip to obtain these properties. The idea here is that the various layers inside VLSI and ULSI devices have different mechanical properties from conventional bulk materials, because the layers are produced as thin films by special processes such as vapor deposition. In order to get accurate results from finite element analysis, accurate material properties are needed. The very small thin film

specimens, with dimensions in microns, are too small to be handled. They must be produced right on the grips, and then tested. The process for producing the specimens and the grips should be compatible with the processes used to produce VLSI and ULSI devices. This can be achieved by micromachining the grips out of silicon using photolithography. Thus, our design has a downward-scalable specimen size, where the specimen is deposited directly on the grips so that no handling is necessary. The two principal technical challenges are to produce the moveable grip, because it is a suspended structure, and to produce a specimen thin film with plane parallel surfaces also suspended in free space.

The brittle-ductile transition and atomic structure in precracked silicon

Recently striking observations by M. Brede and P. Haasen (1988), Y.-H. Chiao and D. Clarke (1989) and P. Hirsh, S. Roberts and J. Samuels (1989) on silicon have shown that even in that brittle solid, dislocations are easily generated at the crack tip. Many of the emitted dislocations are not in the blunting configuration, but in what we will call the jogging and kinking configurations. We have work underway to explore the different effects of these several configurations on dislocation emission; it should give us a better understanding of the conditions under which the change of blunting configuration can give rise to both the activation energy and ductility. Besides the homogeneous nucleation at crack tips, we pursue alternative approaches: one of them is to derive the elastic interaction between cracks and ledges, which are formed by pinned dislocation segments. With these new approaches, we hope to be able to develop a thermally activated model of dislocation emission occurring throughout a zone surrounding the crack tip.

Cleavage, dislocation emission, and shielding for interfacial cracks in bimaterials

Over a number of years, we have established a picture of material ductility in homogeneous single phase solids based on the proposition that material ductility is due, in part, to the atomic configuration of the crack tip and, in part, to the shielding of the crack by external dislocations or other defects. We believe this idea still applies to interfacial cracks in bimaterials.

In an atomic theoretical scheme for fracture problems, we have used the lattice-Green's function formalism and tight-binding (TB) electron theory. Particular attention is paid to study the impurity doping or chemical environment effects on the crack extension process in covalent semiconductor such as silicon. We have constructed a theoretical model for the crack growth by supposing that the atoms of the crystal can be divided into those whose bonds are stretched only into their linear ranges and those whose bonds stretch in the nonlinear range. Under a general overlap repulsive potential, the bond breaking force in silicon is changed considerably (~20%) by the impurity doping and the effect can be detected by careful experiments.

In the role of mismatching elastic constants on the interfacial fracture strength of polycrystalline and multiphase solids, we have studied the stress potential functions for the interaction between dislocations and interfacial cracks in bimaterials. For mode III cracks, the derived dislocation shielding relation is well expected. At the same time, we have shown that the enhancement of dislocation emission in the relative soft solid phase can result from the reduction of image force on the dislocation, and we hope to apply these results to the problems arising in electronic materials and their packaging, and involving multilayer systems, thin films and metal/ceramic or ceramic/ceramic interfaces.

Safety of Structures and Vessels

Stress relief criteria for naval steam pressure vessels

As part of our investigation of the need for stress relief of repair welds in Navy pressure vessels, we completed wide plate tests of repair-welded manganese-molybdenum and carbon steels. The wide plate tests provide data on the crack driving force as a function of imposed load and displacement in a simulated repair weld. Small specimen tests were used to measure the fracture toughness at a variety of locations in and around the weld and its heat-affected zone. Due to the difficulty of precisely locating the crack relative to the weld microstructure in a wide plate, the crack in the wide plate did not sample the most brittle region of the weld. Thus, the wide plate test did not simulate the worst-case conditions. However, one Mn–Mo steel plate did fail catastrophically, and the three others showed crack blunting and crack extension. Good agreement between the small specimen tests and the wide plate tests was observed, in that the degree of blunting or crack growth observed after the wide plate tests matched those observed in the small specimens at comparable J-integral levels.

Missouri pipeline failure

We contributed to the NIST investigation of an oil pipeline failure in Missouri. We visited the control center of the pipeline, where the procedures for starting and stopping the pumps and monitoring the pipeline pressure were observed. Also, we visually examined the failed pipe section. Our assignment was to review the Battelle investigation of the failure. We concluded that the origin had indeed been found by the investigators, and that their conclusions appeared to be supported by their observations. We suggested a more extensive investigation including especially fracture toughness testing and stress analysis of the pipeline, which would be required to positively identify the cause of the failure.

The Cryogenic Materials and Physical Properties Groups investigate the behavior of materials at low temperature and measure and model the properties of advanced materials, including structural alloys, conductors, composites, ceramics, and superconductors.

Cryogenic Materials

Richard P. Reed
Group Leader

E. S. Drexler, W. Fehringer, M. Harzenmoser *, L. Ma,†, J. D. McColskey, C. N. McCowan, P. T. Purtscher, N. J. Simon, R. L. Tobler, P. Turner, R. P. Walsh

We study the mechanical, physical, and metallurgical properties of materials in the temperature range 4 to 295 K. Goals of our research are the characterization and development of metals, alloys, and composites; the development of testing procedures and standards; and the collection and evaluation of material properties data.

A major program in recent years has been the development of materials technology to design and build superconducting magnets for fusion-energy systems. We have expertise in and unique facilities for measuring tensile, shear, creep, and fatigue properties at very low temperatures. We contribute to design and safety assessments, and consult on material selection and properties for a wide range of cryogenic projects.

Representative accomplishments

- Development of a model to characterize the near-adiabatic conditions at low temperatures during mechanical property testing.

---

* Guest worker from the Swiss Federal Institute (ETH), Zurich, Switzerland
† Guest worker from the Institute of Metals, Shenyang, China.

- Design and construction of a unique metric-ton-load-capacity facility for tensile and compression testing at temperatures as low as 4 K.
- Comprehensive study of the creep of copper at 295, 76, and 4 K.
- The properties of aluminum-lithium alloys and copper from over two hundred documents were added to our data base on cryogenic materials and provided to the aerospace community.

Cryogenic Data Compilation and Evaluation

Currently, we are compiling data to support the cryogenic tankage design for the joint Air-Force-NASA Advanced Launch System (ALS). Use of advanced Al–Li alloys is under consideration for this new generation of space vehicles, because of potential savings in launch weight and manufacturing costs. NIST is compiling the existing mechanical and thermal property data for the Al–Li alloys 2090, 8090, and a proprietary grade. These properties will be compared with those of the conventional Al alloy 2219 that was used in construction of the huge external tank of the space shuttle. The effort to date has uncovered significant gaps in the data available; for example, a lack of tensile and fracture data at 20 K, the operating temperature of the liquid hydrogen tank, and a scarcity of cryogenic data as a function of orientation angle, which is important because of the high degree of anisotropy. The NIST effort is carried out in cooperation with the major contractors. NIST recently hosted an Al–Li alloys workshop in Boulder with contractors, alloy suppliers, and Air Force and NASA personnel attending. NIST reported data compilation results at the workshop, and also the results of recent cryogenic tensile and fracture toughness measurements at NIST on new, state-of-the-art commercial heats of these alloys that have started to fill some of the gaps in the database.

In contrast to the work on Al–Li alloys, in which much was accomplished in a three-month period to respond to the rapid development of the ALS program, an ongoing effort has been underway to prepare handbook pages on cryogenic mechanical, thermal, and electrical properties of high purity copper and copper alloys. Much of this data has been available in the literature for many years, but had not been brought together in a useful format. For example, Figure 15 shows the compilation of all available data on the magnetoresistance of C10100–C10700 coppers. A predictive equation has been developed to represent average magnetoresistance from 4 to 300 K. Copper and copper alloys are used as conductors and conductor stabilizers in high-field magnets for prototype fusion reactors. This work is supported by the DoE's Office of Fusion Energy. In addition, many requests for information have been received from designers working on applications in space, military, and high-energy accelerators. Because accurate knowledge of material properties in the cryogenic temperature range may stimulate new uses for copper, a cooperative program with the International Copper Research Association, Inc., is under consideration. This would allow for wider dissemination of the property compilation.

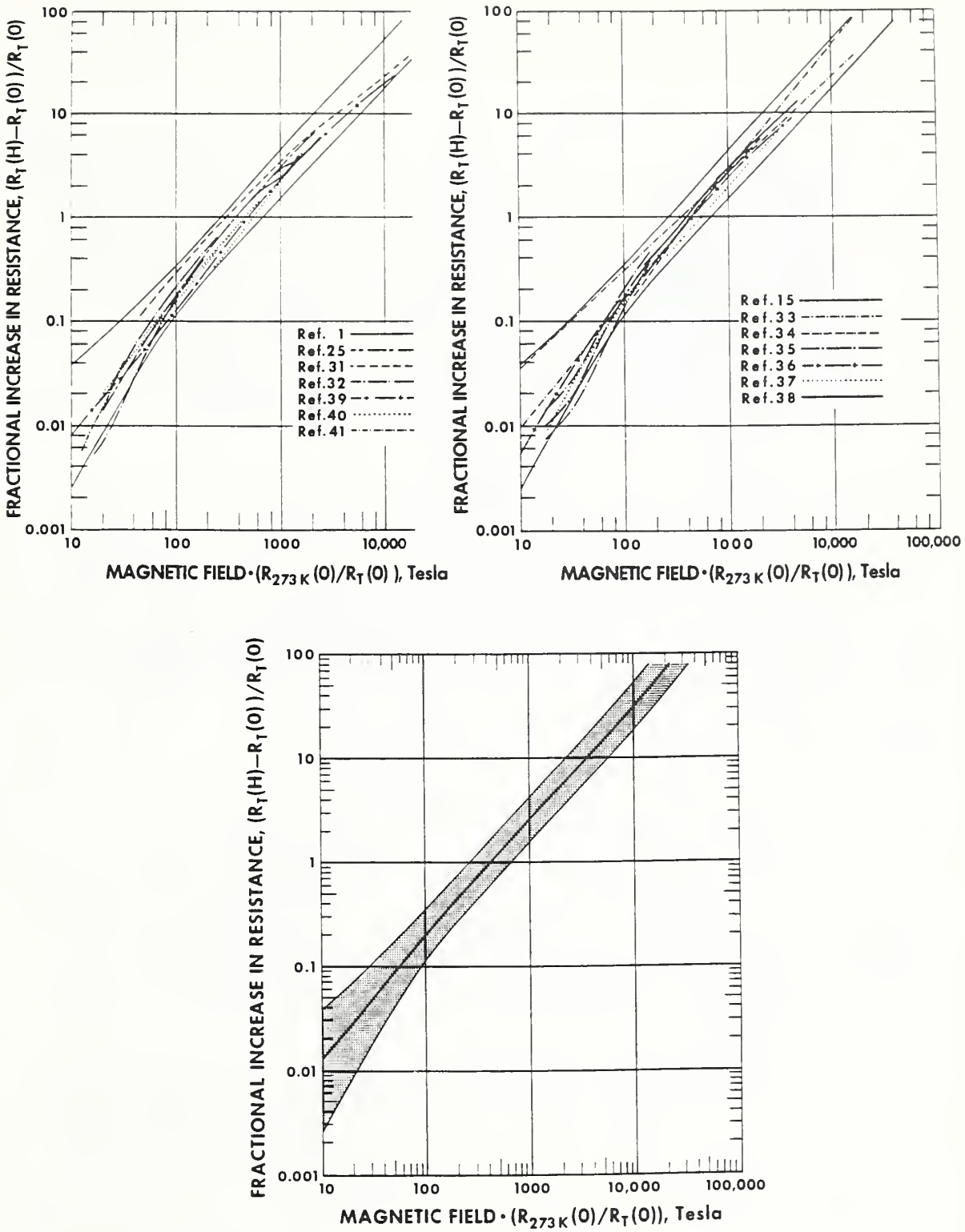

Figure 15. Magnetoresistance of copper. The compiled data sets are represented by the dashed lines in the upper graphs; the lower figure shows the recommended curve and expected uncertainty.

Standards for Structural Metals

NIST, in cooperation with Japanese organizations and the American Society for Testing and Materials (ASTM), continues to develop standard test methods for measuring the tensile and fracture properties of structural alloys at liquid helium temperature. Special considerations apply to mechanical tests near absolute zero because of severe adiabatic heating during plastic deformation. Sponsors of the program are the U.S. Department of Energy, Office of Fusion Energy, and the Japan Atomic Energy Research Institute (JAERI). The program includes personnel exchanges, interlaboratory testing, and individual or cooperative research. Contributing organizations include NIST, four other American laboratories, JAERI, and six other Japanese laboratories.

During this program, which started in 1986, cryogenic materials scientists were interviewed at government, industrial, and academic institutions. International workshops were held in Sendia (March 1986 and January 1987), Reno (October 1986), and Tokai-mura (August 1986 and May 1988). Three interlaboratory test programs were completed. At this time, the eighth draft of the proposed 4-K standard for tension testing of structural alloys has advanced half-way through ASTM's balloting process; official ratification is expected within one year. The 4-K fracture standard was substantially improved after submission to ASTM; its ratification is expected within two years.

Standards for Composites

The present status of mechanical property standards for composites, even at room temperature, is complicated. Industry and government have developed their own standards for specific purposes, and multiple standards have been developed for certain property measurements. For example, the American Society for Testing and Materials (ASTM) now has three separate standards for compression testing, and three more are in process. However, the existing standards do not necessarily address the current needs to establish low temperature standards for filament-reinforced structural composites that are used primarily as electrical insulation in superconducting magnets.

This year, we initiated work on cryogenic standards for composites for the first time. The 1989 program included efforts to cooperate with other standards organizations. We organized an international symposium to clarify the state-of-the-art in low temperature mechanical testing and began to develop cryogenic apparatus and test methodologies for shear and compression testing which are of immediate interest.

We designed an improved apparatus for cryogenic experiments at NIST. Interchangeable fixtures used with this apparatus will enable tension, compression, or shear tests of various types of specimens. A double-notched compact specimen was identified as a promising configuration for cryogenic shear testing.

Physical Properties

Hassel Ledbetter
Research Leader

M. W. Austin, S. A. Kim, M.Lei*, S.-H. Lin§, R. R. Rao†, M. Saito‡

Our research on deformation emphasizes measurements and modeling of elastic constants and related physical properties of metals, alloys, composites, ceramics, and the new oxide superconductors. For many studies, the temperatures range between 295 and 4 K. The elastic constants, which relate deformation to stress, sustain our interest because they relate to fundamental solid-state phenomena: interatomic potentials, equations of state, and phonon spectra. Furthermore, thermodynamics links elastic constants with specific heat, thermal expansivity, atomic volume, and the Debye temperature.

Representative accomplishments

- Considering f.c.c. elements and alloys, we discovered a discontinuity in the bulk-modulus/electron-density relationship (B versus n). As expected from a free-electron model, B first increases with n, but then decreases sharply at a critical value, n_c. Below n_c materials show paramagnetism; above n_c they show either ferromagnetism or antiferromagnetism. This discontinuous behavior provides a chance to understand Fe–Cr–Ni-alloy elastic-constant peculiarities. Furthermore, it provides a possible basis for developing alternative invar (low-thermal-expansion) alloys.

---

* Graduate student from the Institute of Metal Research, Shenyang, China.
§ Graduate student from Physics Department, Tsinghua University, Beijing, China.
† Visiting scientist from the Indian Institute of Technology, Madras, India.
‡ Visiting scientist from Tsukuba University, Ibaraki, Japan.

- Considering voids in ceramics (especially Al_2O_3), we performed elastic-constant modeling calculations. Unlike almost all alternative models, theirs considers void shape: disc, sphere, rod. They concluded that the voids behave like oblate spheroids with a 1:9 aspect ratio. Such spheroids cause a large elastic-constant change. For example, for ten-percent voids, the Young modulus decreases about thirty-two percent; spherical voids cause an eighteen-percent decrease.

- By ultrasonic methods, we confirmed the very different low-temperature phonon behavior of the oxide superconductor $La_{1.85}Sr_{0.15}CuO_4$ and its nonsuperconducting base material La_2CuO_4. Large, irregular, nonhysteretic elastic-constant changes with temperature suggest a magnetically driven second-order phase transition above T_c, the superconducting critical temperature. Near T_c, there appears a minimum in elastic stiffness.

Austenitic steels

On these materials, we completed six elastic-constant and related-property studies.

1. Nickel effect on elastic constants of Fe–Cr–Ni alloys. Using a kilohertz-frequency standing-wave method, we determined the effect of Ni content on the elastic constants of Fe–Cr–Ni alloys containing nominally 20.3 mass percent Cr. Nickel varied from 6.1 to 11.8 mass percent. As expected, we found little change. For example, for five alloys, the Young modulus averaged 196.1 ± 1.7 GPa. Similarly, the shear modulus averaged 77.3 ± 0.4 GPa. Internal friction measured both in extension and torsion showed no systematic composition dependence. The small elastic-constant changes agree with deductions based on atomic size. However, the small decrease in bulk modulus and accompanying increase in shear modulus deserved focus, which we provided by using a Ducastelle model for transition-metal alloys. The model contains two terms: bandstructure and ion-core-repulsion.

2. Elastic constants of four Fe–Cr–Ni–Mn alloys. Using ultrasonic methods, we measured the complete polycrystalline elastic constants of four alloys. Combining these results with those reported previously for five similar alloys, we focused on the alloying effects of chromium, nickel, and manganese. The alloys contain 16 to 23 atomic percent chromium, 7 to 28 atomic percent nickel, and 0 to 13 atomic percent manganese. Only Mn produced regular effects, consistent with volume changes. Both Cr and Ni produced surprising increases in the bulk modulus and equally surprising decreases in the shear modulus. We hypothesize that changing the bonding electrons from d-character to s-character explains such irregularities. We fitted the measurements to Ducastelle's model.

3. Nitrogen effect on elastic constants of f.c.c. Fe–18Cr–19Mn alloys. Previously, we studied effects of interstitial carbon-plus-nitrogen on the elastic constants of f.c.c. Fe–18Cr–10Ni–1Mn alloys. Consistent with a volume increase, all the elastic stiffnesses decrease with increasing C+N. The present alloys show different behavior: even though volume increases, interstitial nitrogen atoms increase the bulk modulus. We found that 3d-electron elements show a peculiar bulk-modulus–electron-concentration behavior (B versus n_e). At first B increases with increasing n_e; beyond a critical concentration, B decreases rapidly. Applying Ducastelle's model shows that interstitial nitrogen increases the bandstructure contribution to the bulk modulus.

4. Low-temperature phase and magnetic interactions in face-centered-cubic Fe–Cr–Ni alloys. We studied the magnetic properties of a set of nine isostructural face-centered-cubic Fe–Cr–Ni alloys by SQUID magnetometry, neutron diffraction, and ultrasonic techniques from 5 to 300 K. Type-1 antiferromagnetic ordering occurred below the Néel temperature (T_N). The dc susceptibility [$\chi(T)$] failed to exhibit a simple Curie–Weiss dependence. Above T_N, $\chi(T)$ contained a temperature-independent component (χ_0): $\chi(T) = \chi_0 + C/(T + \theta)$. The lattice parameter (a) systematically influenced T_N, which decreased from 47.9 ± 0.05 to 35.0 ± 0.5 K as a increased only 0.25%. The average magnetic moment, ≃ 0.5 μ_B, obtained from neutron scattering was lower than the ≃ 1.0 μ_B value obtained from the SQUID measurements. Mean-field estimates of the antiferromagnetic first-neighbor exchange interaction (J_1) and the ferromagnetic second-neighbor interaction (J_2) indicated that $|J_2/J_1| \simeq 1.5$. We take this as evidence for RKKY interaction and argue self-consistently that only the external d electrons are responsible for the localized average moment. This may mean that s–d hybridization of the external electrons is weak in these alloys.

5. Low-temperature magnetic-elastic anomalies in f.c.c. Fe–Cr–Ni alloys. Using ultrasonic methods, we measured the complete elastic constants of several polycrystalline face-centered-cubic Fe–Cr–Ni alloys at low temperatures: 4–295 K. The alloys represent nine interstitial (carbon-plus-nitrogen) compositions. We also measured d.c. magnetic susceptibility. Upon cooling, a paramagnetic–antiferromagnetic (Néel) phase transition occurs. The Néel transition temperature depends strongly on interstitial content. We fit both composition and temperature effects to Ducastelle's 3d-electron model.

6. Low-temperature thermal expansion of Fe–Cr–Ni alloys with various C+N contents. Using x-ray diffraction, we measured between 295 and 5 K the unit-cell size of several Fe–Cr–Ni alloys containing nominally 19Cr and 10Ni (mass percent). The alloys contained various carbon-plus-nitrogen interstitial levels: 0.69 to 1.47 atomic percent. Two facts motivated our study. First, below 100 K these alloys undergo paramagnetic–antiferromagnetic transitions that affect physical properties, especially elastic constants, which relate strongly to atomic volume. Second, studies on γ-iron particles (which share the

same crystal structure, atomic volume, and approximate Néel temperature (T_N) as our alloys) show a 0.3% volume increase during cooling through the Néel transition. For the alloyed, within our measurement error (0.05%), we failed to find a volume change at T_N. Nor did we detect a departure from cubic symmetry arising from antiferromagnetic spin alignment. All the alloys fit a simple two-parameter expression for the dilatation $\Delta l/l$.

Composites

On these materials, we completed seven studies: one plastic-matrix, five metal-matrix, and one ceramic matrix. Some of the studies contain modeling that applies to any occlusion–matrix combination.

1. Internal friction of a glass-epoxy composite. Low-frequency torsional-pendulum measurements showed four mechanical-loss peaks, all attributable to the epoxy matrix. Thus, we failed to find a fiber-matrix-interface contribution.

2. Cast-iron elastic constants: effect of graphite aspect ratio. We gave the first successful model to explain why nodular-graphite cast iron is approximately twice as stiff as flake-graphite cast iron.

3. Elastic constants of SiC_p/Al: measurements and modeling. We found good measurement-modeling agreement for SiC_p volume fractions up to fifty-five percent. Against expectation, internal friction increased with increasing volume fraction.

4. Thermal expansion of an SiC-particle-reinforced composite. For a thirty-volume-percent material, we measured the anisotropic thermal expansion. Existing models gave fair agreement with measurement. There exists an obvious need for better models.

5. Elastic constants of a graphite-magnesium composite. We measured the five independent (transverse-isotropic-symmetry) elastic constants. Using an inverse model, we deduced the complete set of graphite-fiber elastic constants.

6. Fiber-reinforced composites: models for macroscopic elastic constants. We reviewed this subject, and emphasized our recent studies.

7. Elastic constants of porous ceramics. Focusing on aluminum oxide, we considered the relationship between void content, void shape, and lowered elastic stiffness. We concluded that the voids behave as oblate spheroids with a 1:9 aspect ratio.

Superconductors

On these materials, we completed nine studies. The materials included La–Sr–Cu–O, Bi–Sr–Ca–Cu–O, and Y–Ba–Cu–O.

1. Low-temperature elastic constants of polycrystalline La_2CuO_4 and $La_{1.85}Sr_{0.15}CuO_4$. Using ultrasonic methods, we measured the 295–4-K elastic constants. These materials show two elastic-constant similarities: nearly the same ambient-temperature elastic constants and an elastic-stiffness minimum in the 20–40-K region. Their principal difference is that La_2CuO_4 softens 3% during cooling, while $La_{1.85}Sr_{0.15}CuO_4$ softens 30%. This reversible wide-temperature-range softening resembles a magnetic phase transition. Perhaps it relates to the large drop in spin-excitation intensity found by Shirane and coworkers using inelastic neutron scattering.

2. Specific heat of the high-T_c superconductor $(Bi_{1.66}Pb_{0.34})Ca_2Sr_2Cu_3O_{10}$. We measured the specific heat for H = 0 and 7 T in the ranges 0.4 to 20 K and 65 to 125 K. The coefficient of the low-temperature linear term in C was 0 ± 0.5 mJ/K^2· mole. On initial cooling, an anomaly was observed at T_c; but there were dramatic temperature hysteresis effects.

3. Elastic constants of the polycrystalline Bi–Pb–Sr–Ca–Cu–O superconductor. We measured the 5–295-K elastic constants: shear modulus (G), Young modulus (E), bulk modulus (B), and Poisson ratio (ν). Both G and E show nearly normal temperature variation. During cooling, B softens between 215 and 65 K. The Poisson ratio decreases abruptly at 215 K and decreases almost five percent in the 295–5-K region. In its temperature dependence, this compound resembles $YBa_2Cu_3O_7$. However, it shows much lower elastic stiffness. Corrected to the void-free state, we calculate a Debye temperature of 312 K, versus 436 K for $YBa_2Cu_3O_7$. The Poisson ratio, 0.20, agrees well with that of $YBa_2Cu_3O_7$, 0.21. We used Kresin's model to interrelate Debye temperature, critical temperature, and electron-phonon interaction parameter for four classes of copper-oxide superconductors.

4. Hysteretic phase transition in $Y_1Ba_2Cu_3O_{7-X}$ superconductors. We studied ultrasonic-wave velocities, both longitudinal and shear, in $Y_1Ba_2Cu_3O_{7-X}$, between 5 and 295 K, during both cooling and warming. Both waves, especially the longitudinal, show thermal hysteresis. The results suggest a hysteretic phase change that occurs between 160 and 70 K during cooling and between 170 and 260 K during warming. This phase-change hypothesis explains anomalies in several physical properties. The phase change agrees with thermodynamic-instability predictions. We confirmed the hysteresis in Ho–Ba–Cu–O, where it is smaller than in Y–Ba–Cu–O, and in Eu–Ba–Cu–O, where it is larger. In a companion perovskite, $BaTiO_3$, we observed zero hysteresis. At T_c, 91 K, sound velocities show no measurable change in either magnitude or slope. This continuity disputes the current popular view that, contrary to thermodynamics, elastic stiffness increases upon cooling through T_c into the superconducting state. We believe that stiffening results from the usual thermal effects after a phase transformation from a stiffer phase.

5. Grüneisen Parameter of $Y_1Ba_2Cu_3O_7$. Contrary to reports that the Grüneisen parameter of $Y_1Ba_2Cu_3O_7$ is approximately 3.0, we argued that this parameter is approximately 1.5, a value consistent with metal oxides. We offered three arguments. One depends on a lower bulk modulus (B), near 101 GPa, than found in high-pressure X-ray diffraction studies, which yield bulk-modulus values up to 200 GPa. The second depends on an ionic-crystal-model calculation of the Grüneisen parameter. The third depends on the Anderson–Grüneisen parameter determined by measuring dB/dT.

6. Is $Y_1Ba_2Cu_3O_7$ stiff or soft? Using several measured and calculated physical properties, we argue that the high-T_c metal-oxide superconductor $Y_1Ba_2Cu_3O_7$ is elastically soft compared with $BaTiO_3$ or $SrTiO_3$. We conclude that the bulk modulus equals approximately 100 GPa, despite several high-pressure x-ray–diffraction studies that report values up to approximately 200 GPa. Part of the argument uses an ionic-crystal-model calculation of the bulk modulus.

7. Madelung potentials and valences in $Y_1Ba_2Cu_3O_7$ superconductor. Using Ewald's method, we calculated the ion-site potentials and Madelung energy of $Y_1Ba_2Cu_3O_7$ (orthorhombic, Pmmm, No. 47). We considered the effects of copper-ion and oxygen-ion valences. Among seven possible copper–oxygen ion-charge configurations, only two give a low electrostatic bonding energy to agree with oxygen vacancies on 01 sites. Only one configuration supports soft vibrational modes at the Cu2 site. This configuration also represents the lowest total ionic bonding energy.

8. Elastic stiffness of metal-oxide superconductors. We review the elastic constants, especially the Young modulus, of the new copper-oxide superconductors discovered in 1986. We give some results for copper oxides of La, Y, Bi, and Tl. To compensate for fragmentary and contradictory measurement results, we emphasize the relationship to other, simpler oxides and the role of model calculations. We describe elastic-constant interrelationships, corrections to the void-free state to get intrinsic elastic constants, and elastic-constant temperature dependence.

9. Elastic constants, Debye temperatures, and electron–phonon parameters of superconducting cuprates and related oxides. Using both measurements and modeling, we studied the cohesive and related properties of several oxides. Superconducting oxides include $SrTiO_3$, $La_{1.85}Sr_{0.15}CuO_4$, $Y_1Ba_2Cu_3O_7$, and $(Bi–Pb)_2Sr_2Ca_2Cu_3O_{10}$. Related nonsuperconducting oxides included $BaTiO_3$ and La_2CuO_4. For these materials, we gave the complete quasiisotropic elastic constants corrected to the void-free state. From elastic constants and atomic volume, we calculated Debye characteristic temperatures, θ_D. Using Kresin's model, valid for all values of the electron–phonon parameter, λ, we estimated λ from T_c and θ_D. For the superconducting cuprates,

λ ranges from 0.92 (La–O) to 7.96 (Tl–O). Except perhaps for Tl–O, these parameters fall within a range predicted by theory. For all the above materials, we showed the 295–5-K variation of Θ_D. We supported our elastic-constant measurements with Born-model calculations of the bulk modulus.

Other studies

In this category, we mention five elastic-constant-related studies.

1. Thermoelastic coefficient and its pressure derivative: derivation from a Mie–Grüneisen interatomic potential. We derived a relationship for the thermoelastic coefficient $K = -(1/T)(\partial T/\partial\sigma)$, the temperature change caused by stress, and for the thermoelastic-coefficient pressure derivative, $(1/K)(\partial K/\partial P)$. The latter, related to third-order and fourth-order elastic constants, relates simply and approximately to the bulk-modulus temperature derivative, $(1/B)(\partial B/\partial T)$. Comparison with a solid-mechanics model shows agreement within approximately twenty percent.

2. Fourth-order elastic constants of β-brass. We calculated fourth-order elastic-constant combinations by using measured second-order and third-order elastic constants and the expressions for the effective elastic constants of a cubic crystal obtained from finite-strain theory. The calculations show that the Cauchy relations fail. This implies that noncentral or many-body forces occur in this material. We considered two alloys. The higher-Zn alloy shows lower magnitudes of the fourth-order elastic constants and a larger Cauchy discrepancy.

3. Monocrystal–polycrystal elastic-constant models. Considering only cubic symmetry (three independent monocrystal elastic-stiffness coefficients, C_{ij}), we reviewed various models for converting the C_{ij} to the effective macroscopic quasiisotropic and homogeneous elastic constants, usually taken as B, the bulk modulus, and G, the shear modulus. To test the models, we considered a typical metal: copper, which possesses a moderate Zener elastic-anisotropy ratio, 3.19, and which was measured by pulse-echo dynamic (MHz) methods. We found that the Hershey–Kröner–Eshelby, and equivalent, models work best. We ignored models that lack a physical basis. Using the H-K-E model, we calculated the effective polycrystalline elastic constants of twenty-five cubic elements.

4. Resonating-orthotropic-cube method for elastic constants. We describe measurements and analysis that yield, from a single cube-shape specimen, in a single measurement, the complete set of anisotropic elastic-stiffness constants, the C_{ij}. Experimentally, we place a cubic specimen between two piezoelectric transducers, which excite and detect the cube's macroscopic free-vibration (fundamental-mode) frequencies, up to 10 MHz. From the specimen's shape, size, and mass,

and from the measured resonance-frequency spectrum, we analyze for the C_{ij} within a given tolerance ϵ_i:

$$\lambda_i(C_{ij}) - \bar{\lambda}_i = \epsilon_i. \qquad \text{(No sum on i.)}$$

Here $\bar{\lambda}_i$ relates to the measured resonance frequencies, and λ_i represents eigenvalues calculated by a Rayleigh–Ritz method using Legendre-polynomial orthogonality ensures a diagonal mass matrix [m], which simplifies the resulting eigenvalue problem:

$$([k] - \lambda[m])\{x\} = \{0\}.$$

For materials with certain symmetries, the coefficient matrix [k] reduces to a block-diagonal matrix. which reduces computational effort and simplifies vibration-mode identification.

5. Thermal expansivity and elastic constants. We derived a simple, useful relationship between thermal expansion, $\Delta V/V$, and elastic constants. The relationship permits estimation of thermal expansion from only elastic constants (second-order and third-order) and atomic volume. Elastic-constant temperature dependence is not required. We tested the relationship for a variety of crystalline solids. Considering the 0–293-K region, measurement–calculation disagreement ranges from less than one percent to fifteen percent. The model permits extrapolation of high-temperature (near-linear) thermal expansion to zero temperature.

MATERIALS PROCESSING

The Welding and Thermomechanical Processing Groups investigate the non-equilibrium metallurgical changes that occur during processing, such as solidification, recrystallization, phase transformation, and precipitation strengthening. These changes affect the quality, microstructure, properties, and performance of metals. In addition, in FY 1989, we have started a sensor-development effort, which will support our objective of achieving better process controls.

Welding

Thomas A. Siewert
Group Leader

G. Adam,* M. W. Austin, C. N. McCowan, D. A. Shepherd, D. P. Vigliotti

The Welding Group is continuing to study weld flaws, their origins, and their implications on structural performance. Our goals include the development of procedures that reduce the incidence of defects and to develop weld metals with improved tolerance for defects. A long-term goal is to develop a more fundamental understanding of the process of droplet transfer across the arc, then incorporate this information into an intelligent weld controller that improves the quality and efficiency of welding.

Representative accomplishments

- The group has assumed the responsibility for the production of Charpy V-notch calibration specimens for world-wide certification of these machines.
- A prototype radiation-transfer standard has been developed for use as an image-quality indicator for real-time radiology.
- A plasma arc melting procedure has been developed to produce standard reference materials with uniform gas contents for use in calibrating residual gas analyzers.

---

*Guest worker from the Nuclear Research Centre – Negev, Beer-Sheva, Israel.

Arc Physics

With the help of a guest worker, the data collection and processing capability has been upgraded. A digital oscilloscope with a 8-kilobyte memory has been replaced by a 16-MHz microcomputer with 2-megabyte RAM and a 100-kHz A-to-D board. Its larger memory and improved processing capability increase the resolution of transient behavior and the measurement of droplet transfer rate. The utility of this system was demonstrated by evaluating the droplet transfer for a 700 MPa yield strength electrode. Voltage histograms and peak height ratios were found to be useful as control parameters.

The arc-physics equipment in our welding laboratory continues to generate cooperative programs. This year, we published a study on the use of voltage changes as a means of characterizing droplet transfer in gas-metal arc welding. He found that voltage changes greater than approximately 8 V correlated with short-circuiting transfer and voltage changes between 1 and 4 V were associated with globular transfer. Intermediate voltage changes were associated with transitions between these modes, and voltage changes of less than 1 V were associated with spray transfer and electrical noise. These values are consistent with published data and models for voltage drops across the arc. The results provide another sensing methodology for intelligent closed-loop control of welding processes.

Gases in metals

A plasma melting technique is being used to develop standards for residual gas analyzers with uniform gas levels, levels above those attainable by casting techniques. To reduce specimen machining, small spheres are produced by plasma ablation. We are currently evaluating specimens of hydrogen in titanium.

Analyses of fluxes

For many welding processes, the flux is an integral part of the electrode, and it is evaluated during qualification testing. Submerged arc welding is an exception; the electrode and flux come from independent lots. Thus, a flux–electrode combination could be chosen that would not meet the mechanical property requirements even though each had been qualified separately.

In support of standards development, we are evaluating techniques for analyzing welding fluxes. Our goal is to identify a method whereby we can control the flux composition and possibly predict other welding problems.

Charpy V-notch calibration specimens

The most widely used standard for predicting the behavior of steel used in structures and other products has been transferred to the National Institute of Standards and Technology from the U.S. Army Materials Technology Laboratory, Watertown, Massachusetts. The Charpy impact test is a small-scale laboratory fracture experiment that uses a pendulum-type drop hammer and a centimeter-size material specimen to measure the ductile or brittle behavior of steel. Since 1964, the Watertown facility has been providing standard test materials and calibration services, but the program has been transferred to NIST during summer 1989.

The Charpy calibration service consists of V-notched blocks in several energy ranges which are broken in the customer's machine. The data is entered on a form and returned with the specimens. The data is analyzed and acceptable machines will be certified. At present, about 1000 test machines around the world use this service. The Materials Reliability Division and the Office of Standard Reference Materials are cooperating on this program, with OSRM shipping the specimens with a certificate of specimen energy and our Division monitoring the production of the material and certifying the machine results.

Two energy ranges are now in stock, a low energy range (near 17 J) and a high energy range (near 98 J). A higher energy range (near 160 J) is planned for 1990. We are evaluating new materials for other energy ranges and for more consistent values in the existing ranges.

Stainless Steel

In a cooperative program with the Welding Research Council, a diagram was developed that predicts the ferrite content of stainless steel welds with more accuracy than previous prediction diagrams. In the past year, this diagram was submitted to the International Institute of Welding for further evaluation. The Austrian Delegation reported data on over 200 welds that confirms the improved accuracy of the new diagram. At the 1989 Annual Assembly, the IIW voted to request that the new diagram be incorporated in the American Society of Mechanical Engineers Boiler and Pressure Vessel Code, where it will become the standard method for the prediction of ferrite content.

In support of Department of Energy cryogenic applications, we have been evaluating the various stainless steel electrodes and cataloging their mechanical properties. This year three electrodes were evaluated, of compositions 15Cr-35Ni, 20Cr-25Ni-5Mo, and 16Cr-18Ni. All three electrodes were for gas metal arc welding and were fully austenitic. These standard electrodes were welded with special shielding gases, specifically we added nitrogen to argon to increase the strength at cryogenic temperatures and carefully excluded oxygen to increase the toughness. The 16Cr-18Ni

composition produced welds with unacceptable levels of hot cracking, but the other two electrodes produced sound welds with strength and toughness values that exceed those of the leading base metal (type 316LN) and most weld compositions.

Real-time Radioscopy

This topic reflects the desire of U. S. industry to eliminate the costs and evaluation delays associated with x-ray film (radiography) and to change to the CRT based systems (radioscopy) that are becoming available. Current image-quality indicators, which were designed for film radiography must be repositioned for each exposure. Thus, with these indicators, we cannot exploit the advantages of real-time systems: dynamic evaluation and rotation of the specimen without repositioning the detector system. New indicators are being developed that can exploit all the advantages of real-time systems. Prototype indicators with one- and two-dimensional symmetry have been produced in copper and nickel versions, and are being evaluated.

A particular subset of these real-time systems can produce planar slices (laminar views) of a three-dimensional structure. In a joint program with the Department of Defense and the NIST Office of Nondestructive Evaluation, we are planning to obtain such a laminography system and evaluate its ability to detect solder joint defects on printed circuit boards. The system has been ordered and is scheduled to be delivered in March 1990. After determining its accuracy and reproducibility on a variety of solder joint flaws, we plan to develop an enhanced finite element modelling package that can relate the inspection results to the service conditions, for a true assessment of its fitness for service.

Thermomechanical Processing

Yi-Wen Cheng
Research Leader

H. I. McHenry, D. A. Shepherd, Y. Rosenthal*

Research in thermomechanical processing uses a deformation-processing simulator built at NIST. We study the metallurgical changes that occur in steels during forging and subsequent cooling. By controlling the temperature–deformation schedules, the cooling after forging, and the subsequent tempering treatment, we are striving to achieve optimum strength and toughness in direct-cooled and direct-quenched forging steels.

Representative Accomplishments

- The NIST thermomechanical processing (TMP) simulator was used to study the high-temperature high-strain rate flow characteristics and transformation kinetics of two direct-cooled microalloyed steels for forging applications.
- Procedures using numerical analysis were established to precisely determine phase-transformation temperatures from the dilation-vs-temperature curves.

Technical Highlights

Continuous-cooling transformation study

Continuous-cooling transformation (CCT) diagrams were established for microalloyed SAE 1141 and 1522 steels. The usefulness of the CCT diagram is to predict the microstructure of a steel after processing, and thus the mechanical properties. The relative position of the phase diagram as shown in Figure 16 is a function of composition and processing. Figure 16 is the CCT diagram of the microalloyed SAE 1141 steel. The dashed line in Figure

*Guest worker from the Nuclear Research Centre – Negev, Beer-Sheva, Israel.

16 is the cooling profile of a production forging. This line coincides with the line at the far right.

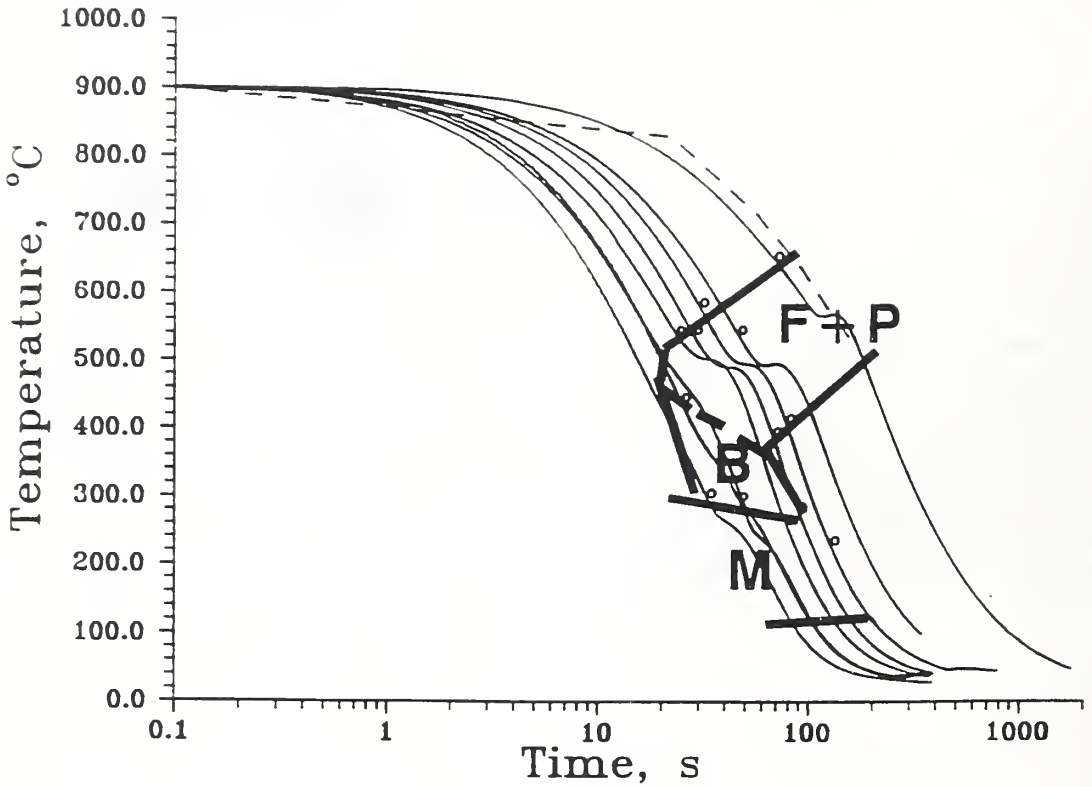

Figure 16. The CCT diagram of the microalloyed SAE 1141 steel. Dashed line is the typical cooling profile found in a forging without forced cooling. F: ferrite; P: pearlite; B: bainite; M: martensite.

Characterization of high-temperature high-strain rate flow property

High-temperature high-strain rate flow characteristics are important in modeling forging and plate rolling. As part of the TMP research, we characterize the flow curves of steels at high temperatures under constant true strain rate. The true stress-vs-true strain relationship is influenced by composition, temperature, strain rate, and deformation history. A representative high-temperature high strain rate flow curve is given in Figure 17.

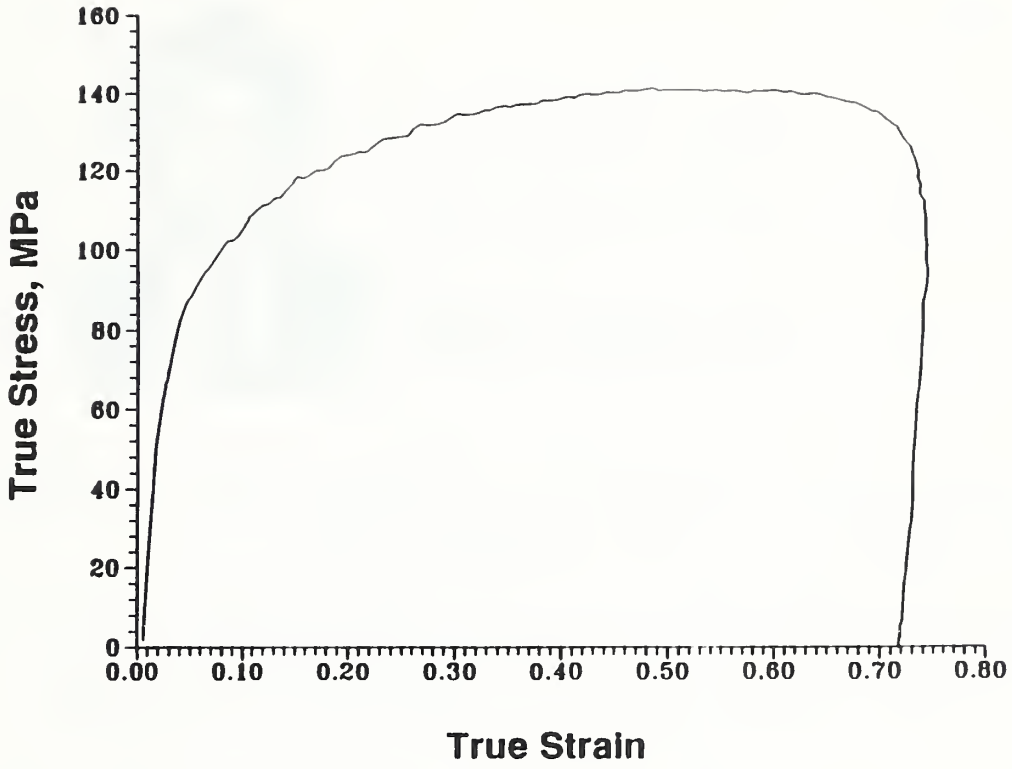

Figure 17. True σ-ϵ characteristic of microalloyed 1522 steel at 1000°C with a compressive strain rate of 10 s^{-1}.

Process Control Sensors

Christopher M. Fortunko
Deputy Division Chief

Mechanization of automated approaches to processing of advanced materials and improving the economy of production of basic materials, such as steel and aluminum, is hampered by the lack of adequate sensors.

The sensor activity represents a new area of emphasis that was started during the last quarter of FY 1989 with the objective of addressing specific measurement needs identified by the industry and to support ongoing in-house research activities in NDE, welding, and thermomechanical processing.

The primary focus of our sensor effort is on measurement techniques that utilize non-contact transducer technologies. Such techniques are particularly appropriate in situations involving elevated temperatures and high production volumes. Our sensor effort is well grounded in existing in-house expertise in the area of non-contact transducers. Among these are electromagnetic-acoustic transducers (EMATs) for texture and weld-quality determination, air-coupled ultrasonic sensors for determining material properties of polymer composites, and microwave and electro optical techniques for accurate displacement measurements.

Representative Accomplishments

- An efficient air-coupled ultrasonic inspection system was demonstrated. The current design is immediately useful for inspecting materials that can be contaminated by the presence of fluid couplants. Examples include certain aerospace materials (foams, honeycombs), electronic materials (solar cells, circuit boards), and advanced materials (high-T_c superconducting ceramics.)

- Steel-industry interest was stimulated in the possibilities offered by microwave sensors for displacement and casting-speed measurement. Optical and laser-based sensors perform poorly in steel-mill environments, because steam and other obscurants effectively block visible radiation and contaminate critical optical-train components. Microwave sensors are generally insensitive to such effects, but can offer measurement accuracy acceptable to the steel and aluminum industries.

Technical Highlights

Our goals are to identify pressing, industry-wide measurement needs and to respond by developing accurate and standardizable measurement techniques. We plan to disseminate the results of our research and development efforts by conducting technology-transfer programs in which the industry would be an active participant. As a part of the technology-transfer programs, the measurement know-how would be transferred to an industrial participant along with an operational sensor prototype system.

Currently, we are focusing our technical resources in the area of sensors that require non-contact transduction methods. Examples of such transducers are:

- electromagnetic-acoustic transducers (EMATs),

- air-coupled ultrasonic transducers,

- microwave and millimeter-wave transducers,

- eddy-current and electrostatic probes, and

- DC and low-frequency current probes.

Air-Coupled Ultrasonic Sensors

Air-coupled ultrasonic transducers are non-contact transducers that can be used to generate and receive MHz ultrasonic signals in many advanced and basic materials. While EMATs are better suited for operation on metals, air-coupled ultrasonic transducers are inherently applicable in the area of polymer-composite materials, foams, etc. Like EMATs, air-coupled transducers require special signal conditioning electronics to realize usable signal-to-noise ratios. However, with proper design air-coupled transducers can facilitate the design of ultrasonic sensors for determining material properties and detecting flaws.

Historically, the development of air-coupled sensors has been hampered by inadequate electronics. However, this state of affairs has been changed by the recent development of high-power MOS-FET transistors and the availability of high-quality piezo-electric ceramic materials. Also, other advances in component design and system integration have been made. As a consequence, practical air-coupled ultrasonic systems are now feasible. We feel that such systems will be particularly useful for high-value ceramic and polymer-composite components such as multilayer circuit boards.

With further improvements in electronics, transducers and use of monatomic gases, such as argon, under pressure, it may be feasible to increase the frequency of operation to 25 MHz, or so. Systems operating in this frequency range would exhibit sufficient resolution for inspecting certain electronic packaging materials and subsystems. In particular, they would be sensitive to

sharp surface-breaking flaws that are often missed by liquid-coupled systems, because liquids can fill the void and eliminate ultrasonic contrast.

Another application of air-coupled ultrasonic material characterization systems is in process control of polymer-composite laminates, pultrusions, and foams. In such applications, the out-of-plane and in-plane elastic properties can be measured. This measurement is more difficult using liquid-coupled systems, because the presence of water significantly alters the elastic-wave dispersion characteristics of thin laminates and can saturate porous materials such as foams. This is not the case for air-coupled systems.

In FY 1989, we have placed in operation a 1-MHz, through-transmission, air-coupled ultrasonic system. The practical potential of this system is demonstrated by its ability to transmit sound through a 3 mm thick polymer circuit board with a 40-dB signal-to-noise ratio. A 30-dB signal-to-noise is generally required for a high-quality C-scan image.

With further improvements in the electronics, the signal-to-noise performance of our demonstration, air-coupled system can be increased by 20-30 dB. We are currently working to achieve this goal. This effort is in collaboration with a maker of ultrasonic transducers and a team at Stanford University.

The team is concentrating on the development of better transducers. In particular, they are interested in the use of aerogel and other low-density materials for front-face impedance matching. We are concentrating on the design of the low-noise receive electronics, high-power transmitters, and application development.

Microwave Sensors

We are convinced that microwave-based sensors can provide accurate measurements of plate thickness, displacement, casting speed, and liquid level. All of the above measurements are important to the steel and aluminum industry. Sensors using microwave radiation offer the advantage of better penetration and easier maintenance than sensors using visible radiation of short-wavelength infrared. This potential has been demonstrated in Japan. While the necessary component technologies exist in the U.S., there has been relatively little interest. Perhaps, the practical potential of microwaves has been overshadowed by the dominance of visible-radiation metrology techniques in other industries.

In FY 1989, we conducted a literature search and contacted several individuals at companies engaged in research and development of microwave techniques. We found that a considerable capability in this area exists within Electromagnetic Fields Division at the National Institute of Standards and Technology in Boulder. In particular, the 6-port technology, which is used by the Japanese to provide accurate displacement measurements, has been developed largely at NIST. In the future, we plan to tap this expertise to address selected measurement needs of the U.S. steel and aluminum industries.

Also in FY 1989, to stimulate industry interest in microwave sensor techniques, we took an active role in the joint NIST/AISI/DoE workshop on intelligent processing for primary metals. In response to the positive reaction from the industrial participants, we are currently exploring the possibility of conducting exploratory work in this area in FY 1990.

OUTPUTS
and
INTERACTIONS

SELECTED RECENT PUBLICATIONS*

1. Adam, G.; Siewert, T. A., On-line arc welding data acquisition and analysis system, to be published by ASM in Advances in Welding Science and Technology, 1989.

2. Adam, G.; Siewert, T. A., Sensing of GMAW droplet transfer modes for a Mil 100S-1 electrode, submitted to Welding Journal.

3. Adam, G.; Siewert, T., On-line arc welding data acquisition and analysis using a high level scientific language, Intelligent Instruments and Computers, 1989, 14.

4. Auld, B.A.; Moulder, J.C.; Jefferies, S.; Shull, P.J.; Ayter, S.; Kenney, J. Eddy current reflection problems: Theory and experiment. J. Res. Nondestruct. Eval., Vol. 1, No. 1, 1989.

5. Austin, M. W.; Ledbetter, H. M., Low-temperature thermal expansion of Fe–Cr–Ni alloys with various C+N contents, submitted to Materials Science and Engineering.

6. Berger, J. R.; Dally, J. W., A spatially overdetermined analysis for propagation toughness using strain gages, submitted to Mechanics Research Communications.

7. Berger, J. R.; Kriz, R.D., An improved optical diffraction strain analysis system, Proceedings, 1989 SEM Spring Conference on Experimental Mechanics, Cambridge, MA, pp. 572–578.

8. Berger, J. R.; Dally, J. W.; Sanford, R. J., Determining the dynamic stress intensity factor with strain gages using a crack tip locating algorithm, submitted to Eng. Fract. Mech..

9. Cheng, Y.-W.; Y. A. Rosenthal; McHenry, H. I., Development of a computer-controlled hot-deformation apparatus at NIST, NISTIR 89-3985, 1989.

10. Cheng, Y.-W.; McHenry, H.I., A hot-deformation apparatus for thermomechanical processing simulation. Accepted for publication in Proceedings of the International Symposium on Physical Simulation of Welding, Hot Forming, and Continuous Casting.

11. Clark, A. V.; Thompson, R. B.; Blessing, G. V.; Matlock, D., Ultrasonic measurement of formability in thin ferritic steel sheet, Review of Progress in Quantitative Nondestructive Evaluation, Vol. 8A, D. O. Thompson and D. E. Chimenti, eds., Plenum, New York, 1989, 1031.

---

*Papers that were published or accepted for publication by the Editorial Review Boards of the National Institute of Standards and Technology during fiscal year 1989.

12. Clark, A. V.; Thompson, R. B.; Reno, R. C.; Blessing, G. V.; Matlock, D., Ultrasonic measurement of sheet anisotropy and formability, Proceedings, Society of Automotive Engineers Symposium, 1989, published as part of Sp-779-Steel Stamping Technology: Applications and Impact, 1989.

13. Dally, J. W.; Berger, J. R.; Ham, Kyoung-Chun, On the use of birefringent coatings in fracture mechanics, Proceedings of the 1989 SEM Spring Conference on Experimental Mechanics, Cambridge, MA, pp. 513–520.

14. Datta, S. K.; Ledbetter, H. M., Fiber-reinforced composites: models for macroscopic elastic constants, ASTM STP 1045, Dynamic Elastic Modulus Measurements in Materials, in press.

15. Delsanto, P. O.; Mignogna, R. B.; Clark, A. V., Ultrasonic texture and stress measurements in anisotropic polycrystalline aggregates, submitted to J. Acoust. Soc. Amer..

16. Dodds, R.H., Jr.; Read, D.T. Experimental and numerical studies of the J-integral for a surface flaw. Submitted to Int. J. Fract..

17. Fields, R. J.; Pugh, E. N.; Read, D. T.; Smith, J. H., An assessment of the performance and reliability of older ERW pipelines, NISTIR 89-4136, National Institute of Standards and Technology, 1989.

18. Fisher, R. A.; Kim, S.; Wu, Y.; Phillips, N. E.; Ledbetter, H. M.; Togano, K., Specific heat of the high-T_c superconductor, Physica C, Proceedings M^2S-HTSC (Stanford), July 1989, in press.

19. Fitting, D. W.; Clark, A. V., Monitoring of anisotropic material elastic properties using ultrasonic receiving arrays, Proceedings, Third International Symposium on Nondestructive Characterization of Materials, to be published by Springer-Verlag.

20. Fitting, D. W.; Kriz, R. D.; Clark, A. V., Measuring in-plane elastic moduli of composites with arrays of phase-insensitive ultrasound receivers, Review of Progress in Quantitative Nondestructive Evaluation, Vol. 8B, Thompson, D.O. and Chimenti, D.E., eds., pp. 1497–1504 (1989), Plenum Press, New York.

21. Heerens, Jürgen; Read, D. T., Fracture behavior of a pressure vessel steel in the ductile-to-brittle transition region, NISTIR 88-3099, 1988.

22. Heyliger, P. R.; Reddy, J. N., A higher order beam finite element for bending and vibration problems, J. Sound Vib., 126, 1988, 309–326.

23. Heyliger, P. R.; Moulder, J. C.; Nakagawa, N., Numerical simulation of flaw detection with a capacitive array sensor using finite and infinite elements, Review of Progress in Quantitative Nondestructive Evaluation, Vol. 8A, Plenum Press, 1989, 1023–1030.

24. Heyliger, P. R.; Kriz, R. D., Stress intensity factors by enriched mixed finite elements. International J. for Numerical Methods in Engineering, Vol. 28, 1989, 1461–1473.

25. Heyliger, P.; Ledbetter, H.; Austin, M., Resonating-orthotropic-cube method for elastic constants, ASTM STP 1045, Dynamic Elastic Modulus Measurements in Materials, in press.

26. Kim, S. A.; Ledbetter, H. M.; Li, Y., Elastic constants of four Fe–Cr–Ni–Mn alloys, submitted to Mater. Sci. Eng..

27. Kohn, G.; Siewert, T.A. Dynamic arc-power source response in GMA welding. Submitted to Weld. J..

28. Kriz, R. D.; McColskey, J. D., Mechanical properties of alumina/PEEK unidirectional composite: compression, shear, and tension, Advances in Cryogenic Engineering, in press.

29. Kriz, R. D.; Heyliger, P. R., Finite element model of stress wave topology in unidirectional graphite/epoxy: wave velocities and flux deviations, Review of Progress in Quantitative Nondestructive Evaluation, Vol. 8A, Plenum Press, 1989, 141–148.

30. Kriz, R. D.; Gary, J. M., Numerical simulation and visualization models of stress wave propagation in graphite/epoxy composites, Review of Progress in Quantitative Nondestructive Evaluation, Vol. 9; in press.

31. Ledbetter, H. M., Low-temperature magnetic-elastic anomalies in F.C.C. Fe–Cr–Ni Alloys, Proceedings ISOMES '89, Physica B, 161, 1989, 91–98.

32. Ledbetter, H. M.; Kim, S. A.; Datta, T.; Estrada, J.; Violet, C. E., Poisson-ratio anomalies in the $Y_1Ba_2Cu_3O_{7-x}$ superconductor. Submitted to Phys. Rev. Lett..

33. Ledbetter, H. M.; Kim, S. A.; Austin, M. W.; Datta, T.; Estrada, J.; Violet, C. E., Low-temperature elastic constants of a $Y_1Ba_2Cu_3O_{7-x}$ superconductor. Submitted to Phys. Rev. B.

34. Ledbetter, H., Grüneisen parameter of $Y_1Ba_2Cu_3O_7$, Physica C 159, 1989, 488–490.

35. Ledbetter, H.; Lei, M.; Kim, S., Elastic constants, debye temperatures, and electron-phonon parameters of superconducting cuprates and related oxides, Phase Transitions, in press.

36. Ledbetter, H.; Kim, S. A.; Violet, C. E.; Thompson, J. D., Low-temperature elastic constants of polycrystalline La_2CuO_4 and $La_{1.85}Sr_{0.15}CuO_4$, Proceedings M^2S-HTSC, Physica C, in press.

37. Ledbetter, H., Elastic stiffness of metal-oxide superconductors, Proceedings, First Internat. SAMPE Sympos. (Tokyo, November 1989), in press.

38. Ledbetter, H. M.; Weller, M., Internal-friction spectrum of a glass-epoxy composite, submitted to J. Mater. Res..

39. Ledbetter, H., Monocrystal-polycrystal elastic-constant models, ASTM STP 1045, Dynamic Elastic Modulus Measurements in Materials, in press.

40. Ledbetter, H. M.; Lei, M.; Datta, S. K., Elastic constants of porous ceramics, submitted to Amer. Ceram. Soc..

41. Ledbetter, H.; Lei, M.; Rao, R. R., Thermoelastic coefficient and its pressure derivative: Derivation from a Mie–Grüneisen interatomic potential, Physica B, 1989, 265–268.

42. Ledbetter, H. M.; Kim, S. A.; Goldfarb, R. B.; Togano, K., Elastic constants of polycrystalline Bi–Pb–Sr–Ca–Cu–O superconductor, Phys. Rev. B. 39, 1989, 9689–9692.

43. Ledbetter, H. M.; Kim, S. A., Hysteretic phase transition in $Y_1Ba_2Cu_3O_{7-x}$ superconductor, Phys. Rev. B, 38, 1988, 11857–11860.

44. Ledbetter, H.; Lei, M., Is $Y_1Ba_2Cu_3O_7$ stiff or soft? J. Mater. Res., in press.

45. Ledbetter, H.; Lei, M., Madelung potentials and valences in $Y_1Ba_2Cu_3O_7$ superconductor, submitted to Physica C.

46. Almasan, C.; Datta, T.; Edge, R. D.; Jones, E. R.; Cable, J. W.; Ledbetter, H. M., Low-temperature phase and magnetic interactions in fcc Fe–Cr–Ni alloys, Journal of Magnetism and Magnetic Materials, in press.

47. Lei, M.; Ledbetter, H. M., Elastic constants of SiC_p/Al: measurements and modeling, Metall. Trans., in press.

48. Lei, M.; Ledbetter, H., Nickel effect on elastic constants of Fe–Cr–Ni alloys, submitted to Mater. Sci. and Eng..

49. Lin, S.; Ledbetter, H., Nitrogen effect on elastic constants of f.c.c. Fe–18Cr–19Mn alloys, submitted to Mater. Sci. and Eng..

50. Lin, I.-H.; Thomson, R.M., Relativistic BCS-OHR model. Proceedings, Seventh International Conference on Fracture, Pergamon, New York, in press.

51. Liu, S.; Siewert, T.A., Metal transfer in gas metal arc welding; droplet frequency. Welding Journal, 1989, 52-S.

52. Liu, S.; Siewert, T. A.; Lan, H.-G., Metal transfer mode in gas metal arc welding, to be published by ASM in Advances in Welding Science and Technology, 1989.

53. Ma, L.; Han, J. K.; Tobler, R. L.; Walsh, R. P.; Reed, R. P., Cryogenic fatigue of high-strength aluminum alloys and its correlations with tensile properties, Advances in Cryogenic Engineering, Vol. 36, Plenum Press, New York, in press.

54. McCowan, C. N.; Siewert, T. A.; Olson, D. L., Stainless steel weld metal: Prediction of the ferrite content, Weld. Res. Counc. Bull., in press.

55. McCowan, C. N.; Siewert, T. A., Fracture toughness of 316L stainless steel welds at 4 K, Advances in Cryogenics Engineering, Vol. 36, Plenum Press, New York, in press.

56. McHenry, H. I.; Denys, R. M., Measurement of HAZ toughness in steel weldments, Fifth International Fracture Mechanics Summer School, Dubrovnik, Yugoslavia. In press.

57. McHenry, H. I., ed., Fracture and Deformation Division technical activities 1988, NISTIR 88-3841, National Institute of Standards and Technology, Washington, D.C.

58. Nakajima, H.; Yoshida, K.; Shimamoto, S.; Tobler, R. L.; Reed, R. P.; Walsh, R. P.; Purtscher, P. T., Round robin tensile and fracture toughness test results for CSUS-JN1 (Fe–25Cr–15Ni–0.35N) austenitic stainless steel at 4 K, Adv. Cryo. Eng.-Mater., Vol. 36, Plenum Press, New York, in press.

59. Purtscher, P.T.; Read, R.P., Influence of interstitial content on fracture toughness, Proceedings of the International Conference on High Nitrogen Steels. London: Inst. Met., eds. J. Foct and A. Hendry, 1989, 189–193.

60. Purtscher, P. T.; Ma, L.-M.; Mataya, M. C.; Reed, R. P., Effect of processing on 4-K mechanical properties of a microalloyed austenitic stainless steel, Adv. Cryo. Eng.-Mater., Vol. 36, Plenum Press, New York, in press.

61. Purtscher, P. T.; Austin, M. W.; McCowan, C.; Reed, R. P.; Walsh, R. P.; Dunning, J., Application of 9% Cr austenitic steels at cryogenic temperatures, Adv. Cryo. Eng.-Mater., Vol. 36, Plenum Press, New York, in press.

62. Rao, R. R.; Ledbetter, H. M., Fourth-order elastic constants of β-brass, Int. J. Thermophys., in press.

63. Read, D. T., Analysis of strains measured during a wide plate crack arrest test, Deutscher Verband für Materialprüfung E.V., Berlin, 1988.

64. Read, D.T.; Pfuff, M., Potential drop in the center-cracked panel with asymmetric crack extension, Submitted to Int. J. Fract.

65. Read, D. T.; McHenry, H. I., Postweld heat treatment criteria for repair welds in 2-1/4Cr–1Mo superheater headers: an experimental study, NBSIR 87-3075, 1988.

66. Read, D. T., Measurement of applied J-integral produced by residual stress, Engineering Fracture Mechanics, Vol. 32, No. 1, 1989, 147–153.

67. Reed, R.P.; Simon, N.J. Nitrogen strengthening of austenitic stainless steels at low temperatures. Proceedings, International Conference on High Nitrogen Steels, London: Inst. Met., 1989, 180–188.

68. Reed, R. P.; Simon, N. J., Discontinuous yielding during tensile tests at low temperatures, Advances in Cryogenic Engineering-Materials, Vol. 36, Plenum Press, New York, in press.

69. Reed, R. P.; Simon, N. J.; Walsh, R. P., Creep of copper: 4 to 295 K, Advances in Cryogenic Engineering-Materials, Vol. 36, Plenum Press, New York, in press.

70. Reed, R. P.; Walsh, R. P.; Tobler, R. L., The effect of strain rate on tensile properties at 4 K of a VAMAS round-robin austenitic steel, Advances in Cryogenic Engineering-Materials, Vol. 36, Plenum Press, New York, in press.

71. Reed, R. P.; Lee, H. M.; Han, J. K., The load-control tensile behavior of austenitic steels at low temperatures, Advances in Cryogenic Engineering- Materials, Vol. 36, Plenum Press, New York, in press.

72. Reed, R. P.; Austin, M. W., Effect of nitrogen and carbon on FCC-HCP stability in austenitic steels, Scripta Metallurgica, Vol. 23, 1989, 1359–1362.

73. Reed, R. P., Nitrogen in austenitic stainless steels, J. Met., Vol. 41, No. 3, 1989, 16–21.

74. Rosenthal, Y. A.; Tobler, T. L.; Purtscher, P. T., J_{Ic} data analysis with a negative crack growth correction procedure, J. Testing Evaluation, in press.

75. Rosenthal, Y. A.; Cheng, Y.-W., Computer programs for the determination of phase transformation temperatures using numerical methods, NISTIR 89-3923.

76. Rosenthal, Y.; Cheng, Y.-W., Computerization of a thermomechanical processing research system, J. Intell. Instrum. Comput., 1989, 58–88.

77. Sanford, R. J.; Dally, J. W.; Berger, J. R., An improved strain gage method for measuring KID for a propagating crack, submitted to J. Strain Analysis for Engineering Design.

78. Sanford, R. J.; Dally, J. W.; Berger, J. R., An improved strain gage method for measuring K_{ID} for a propagating crack, Proceedings of the 1989 SEM Spring Conference on Experimental Mechanics, Cambridge, MA, pp. 655–661.

79. Schramm, R. E.; Clark, A. V., Ultrasonic inspection of railroad wheels using EMATs, NISTIR 88-3906, National Institute of Standards and Technology, Boulder, Colorado, 1988.

80. Schramm, R. E.; Shull, P.J.; Clark, A.V.; Mitrakovic, D.V. EMAT examination for cracks in railroad wheel treads. Submitted to Proceedings of the Nondestructive Testing and Evaluation for Manufacturing and Construction Conference. Washington, D.C.: Hemisphere Publishing.

81. Schramm, R.E.; Shull, P.J.; Clark, Jr., A.V.; Mitrakovic, D.V., Crack inspection of railroad wheel treads by EMATs. Submitted to Proceedings: Third International Symposium on Nondestructive Characterization, 3–6 October, 1988, Saarbrücken, Federal Republic of Germany.

82. Schramm, R.E.; Shull, P.J.; Clark, A.V., Jr.; Mitrakovic, D.V., EMATs for roll-by crack inspection of railroad wheels. Review of Progress in Quantitative Nondestructive Evaluation, Vol. 8A, eds. D.O. Thompson and D.E. Chimenti, Plenum Press, NY (1989), pp. 1083–1089.

83. Shull, P. J.; Clark, A. V.; Heyliger, P. R.; Moulder, J. C.; Auld, B. A., Characterization of capacitive array for NDE applications, Research in Nondestructive Evaluation, Vol. 1, 1989.

84. Shull, P. J.; Clark, A. V.; Heyliger, P.; Auld, B. A., Capacitive array sensor for nondestructive evaluation, Review of Progress in Quantitative Nondestructive Evaluation, Vol. 8A, Plenum Press, 1989, 1013–1021.

85. Siewert, T.A.; McCowan, C.N.; Vigliotti, D.P., Cryogenic material properties of stainless steel tube-to-flange welds. Submitted to Cryogenics.

86. Siewert, T.A.; McCowan, C.N.; Olson, D.L. Prediction of ferrite number to 100 FN in stainless steel welds. Weld. J., Vol. 67, 1989, 289s–298s.

87. Siewert, T. A., Standards for real-time radiography — National Bureau of Standards. Submitted to Proceedings, American Society for Nondestructive Testing.

88. Siewert, T.A., Review of 1986 workshop: Computerization of Welding Information. Submitted to Proceedings of the Second Conference and Workshop on Computerization of Welding Information.

89. Siewert, T. A., Improved standards for real-time radioscopy. Nondestructive Evaluation: NDE Planning and Application, NDE-Vol. 5, the American Society of Mechanical Engineers, New York, NY, 1989, 95–97.

90. Siewert, T. A.; Adam, G., The use of a statistical software package for monitoring material quality, submitted to Intelligent Instruments and Computers.

91. Siewert, T. A.; McCowan, C. N.; Olson, D. L., Ferrite number prediction for stainless steel welds, Chapter in book published by American Society for Metals, in press.

92. Siewert, T. A., Typical usage of radioscopic systems: replies to a survey, Mater. Eval., 1989, 701–705.

93. Tobler, R. L.; Reed, R. P.; Purtscher, P. T., Linear-elastic fracture of high-nitrogen austenitic stainless steels at liquid helium temperature, Journal of Testing and Evaluation, Vol. 17, No. 1, 1989, 54–59.

94. Tobler, R. L.; Han, J. K.; Ma, L.; Walsh, R. P.; Reed, R. P., Tensile, fracture and fatigue properties of notched aluminum alloy sheets at liquid nitrogen temperature, Aluminum–Lithium Alloys, Vol. II, T. H. Sanders, Jr., and E. A. Starke, Jr., Eds., Proceedings of the Fifth International Aluminum–Lithium Conference, Materials and Component Engineering Publications Ltd., Birmingham, England, 1989, 1115–1124.

95. Yukawa, S., Guidelines for pressure vessel safety assessment NISTIR 88-3095, National Institute of Standards and Technology, Boulder, Colorado, in press.

SELECTED TECHNICAL AND PROFESSIONAL COMMITTEE LEADERSHIP

American Society of Mechanical Engineers
- Boiler and Pressure Vessel Code Committee
  - Working Group on Materials, Subgroup on NUPACK, SC III
    - S. Yukawa, Chairman
- *Journal of Applied Mechanics*
  - R. D. Kriz, Reviewer
- Materials and Structures Group
  - S. Yukawa, Immediate Past Vice President

American Society for Testing and Materials
- E07.01: Nondestructive Evaluation
  - Task Force on Evaluation of Real-Time Systems
    - T. A. Siewert, Member
- E24.06.05: Fracture Testing of Welds
  - H. I. McHenry, Chairman
- E28.07: Impact Testing
  - T. A. Siewert, Chairman

American Welding Society
- Technical Papers Committee
  - T. A. Siewert
- *Welding Journal*
  - H. I. McHenry, Reviewer
  - T. A. Siewert, Reviewer
- Conference on Computerization of Welding Data
  - Organizing Committee
    - T. A. Siewert

ASM International
- Joining Division
  - T. A. Siewert, Government Liaison

Colorado School of Mines
- T. A. Siewert, Adjunct Professor
- Advanced Steel Processing and Products Research Center Advisory Board
  - H. I. McHenry

Defense Advanced Research Projects Agency
- Advanced Submarine Technology Program
  - Metals Planning Group
    - H. I. McHenry

International Cryogenic Materials Conference
- Board of Directors
  - R. P. Reed, Finance Officer
- Proceedings
  - R. P. Reed, Coeditor

International Institute of Welding

Task Group for Elastic-Plastic Fracture-Mechanics Standard
D. T. Read

International Union of Theoretical and Applied Mechanics
Organizing Committee
H. M. Ledbetter

Metallurgical Society
Metallurgical Transactions
H. M. Ledbetter

Metals Properties Council
Technical Advisory Committee
R. P. Reed

National Academy of Science
Materials Advisory Group of the Marine Board
T. A. Siewert

NIST-Boulder Editorial Review Board
R. L. Tobler, to May 1989
J. R. Berger

Superconducting Magnetic-Energy Storage
Technical Advisory Group
R. P. Reed

University of Colorado
Department of Mechanical Engineering Graduate Faculty
H. M. Ledbetter, Adjunct Professors

U.S. Department of Energy, Office of Fusion Energy
Analysis and Evaluation Task Group
N. J. Simon
Joint U.S.-Japanese Exchange Program Advisory Committee
R. P. Reed
Low-Temperature Materials for Magnetic Fusion Energy Committee
R. P. Reed, Coordinator
Magnetics Group, Advisory Committee
R. P. Reed

Versailles Project on Advanced Materials and Standards Task Group
Cryogenic Structural Materials Working Group
R. P. Reed

Welding Research Council
Data Base Task Group
T. A. Siewert
Materials and Welding Procedures Subcommittee
T. A. Siewert
University Research Committee
T. A. Siewert

AWARDS

Dr. R. P. Reed was selected Outstanding Scientist/Engineer for 1989 by the Excellence in Government Awards Program of the Denver Federal Executive Board. He was cited for outstanding research on cryogenic materials.

C. N. McCowan and T. A. Siewert received the McKay-Helm Award at the 1989 Annual Meeting of the American Welding Society for a significant contribution to the field of welding with their paper "Ferrite Number Prediction to 100 FN in Stainless Steel Weld Metal."

Dr. T. A. Siewert was elected to the position of Honorary Lifetime Member of the American Welding Society for "eminent service to welding engineering and its allied sciences."

Dr. Yi-Wen Cheng received the Bronze Medal Award of the Department of Commerce for Superior Federal Service. He was cited for his development of a thermomechanical processing simulator which is used to develop metallurgical data on the response of steel to deformation processing.

INDUSTRIAL AND ACADEMIC INTERACTIONS

Industrial Interactions

Alcoa

The Cryogenic Materials Group is evaluating the metallurgical and mechanical properties of two vintages of Al–Li alloys.

AMP

The Cryogenic Materials Group provided a two-week training session to two AMP staff members on measuring mechanical and physical properties at low temperatures.

Bechtel

The Cryogenic Materials Group is conducting large-scale tests on composite materials for use in the superconducting magnetic energy storage system.

Chaparral Steel

Yi-Wen Cheng and Dominique Shepherd are working with Chaparral Steel to determine the influence of processing on the transformation kinetics of a new microalloyed bar steel.

Chrysler Corporation

Yi-Wen Cheng is working with Eaton to develop the metallurgical data needed for the direct forging of microalloyed bar steels.

Conoco

D. T. Read is working with Conoco to develop fiber optic techniques to detect damage in uniaxial composite rods being evaluated for use as tendons in tension-leg platforms.

DuPont

P. J. Shull and A. V. Clark are working with DuPont on the nondestructive evaluation of Kevlar rope.

Eaton Corporation

Yi-Wen Cheng is working with Eaton to develop the metallurgical data needed for the direct forging of microalloyed bar steels.

Ford Motor Company

A. V. Clark is working with Ford to develop an ultrasonic measurement of formability. NIST is developing the instrument and Ford the tooling for use in an on-line demonstration at a Ford stamping plant.

General Atomics

The Cryogenic Materials Group is conducting large-scale tests on composite materials for use in the superconducting magnetic energy storage system.

General Electric

T. A. Siewert is working with the Aircraft Engines Department of General Electric and the Army Materials Technology Laboratory to develop a military standard for radioscopic inspection.

Hercules

P. J. Shull is working with Hercules on the use of eddy-current and capacitive-array probes for nondestructive evaluation of composites.

Lockheed

C. M. Fortunko is working with Lockheed to develop a new standard test block to calibrate transducers used to inspect composite materials.

Lukens Steel

Yi-Wen Cheng is working with Lukens Steel to qualify thermomechanically processed steels for use in Naval shipbuilding.

Martin-Marietta

The Cryogenic Materials Group is generating and compiling mechanical property data on a new Al–Li alloy.

McDonnell–Douglas

J. D. McColskey is measuring the mechanical properties of graphite/PEEK composites, which may be used on the national aerospace plane (NASP).

Newport News Shipbuilding

T. A. Siewert is working with Coldren Consulting Company to develop electrodes for welding high strength steels.

Precision Acoustic Devices (PAD), Inc.

C. M. Fortunko is collaborating with PAD in the development of an air-coupled ultrasonic instrument for the nondestructive evaluation of composite materials.

Perkin Elmer

H. Ledbetter is studying the sound velocities, thermal expansivity, and electrical resistivity of pure beryllium at low temperatures for Perkin Elmer in Danbury, Connecticut. Initial sound-velocity results suggest an unexpected low-temperature transition.

SCM Metal Products

H. Ledbetter is studying the elastic constants of alumina-dispersion-strengthened copper that is manufactured at SCM Metal Products in Cleveland, Ohio. Because the alumina particles are so small (a few hundred angstroms), modeling this material presents an intriguing problem.

Toray Industries (Japan)

H. Ledbetter, with T. Kyono, is studying the elastic constants of graphite-fiber metal-matrix composites.

Union Pacific Railroad

R. E. Schramm is developing an instrument to embed in railroad track to be used for the roll-by inspection of wheels.

Welding Research Council

T. A. Siewert and D. P. Vigliotti assist the Materials and Welding Procedures Committee in the development of prequalified welding procedures. The committee is composed of welding fabricators, inspection agencies, insurance companies, sheet-metal workers, and other representatives of the welding industry. It has produced, inspected, tested, and witnessed welds that meet the requirements of fabrication codes. The data from these welds are the basis for new weld-procedure specifications.

Academic Interactions

Colorado School of Mines

T. A. Siewert is working with H.-G. Lan and S. Liu in the study of droplet transfer in the welding arc.

A. V. Clark collaborates with D. Matlock on texture and formability research using ultrasonics.

Colorado State University

H. Ledbetter collaborates with P. Heyliger (Civil Engineering Department) in studying the natural-resonance frequencies of regular-shape solids.

Davidson College

H. Ledbetter collaborates with L. Cain of the Physics Department at Davidson College in Davidson, North Carolina in experimental studies of elastic constants.

Harvard University

I.-H. Lin started a one-year sabbatical to study the fracture and deformation of electronic materials under the direction of Professor J. R. Rice.

Indian Institute of Technology (Madras)

H. Ledbetter collaborates with R. Rao (Physics) on higher-order elastic constants of various solids.

Institute of Metal Research (Shenyang, P. R. China)

H. Ledbetter collaborates with Y. Li in studying the elastic constants of various f.c.c. Fe–Cr–Ni alloys.

Iowa State University: Center for Advanced NDE, Ames Laboratories

A. V. Clark collaborates with R. B. Thompson on texture and formability using ultrasonics.

R. D. Kriz is working with J. C. Moulder, originator of the technique, to improve an optical-strain-measurement system.

Massachusetts Institute of Technology

I.-H. Lin works with A. Argon in studying the brittle-to-ductile transition in cleavage fracture.

Max-Planck-Institut für Metallforschung (Stuttgart, F. R. Germany)

H. Ledbetter collaborates with M. Weller to study the internal friction and dielectric constants of various materials.

National Research Institute for Metals (Tsukuba, Japan)

H. Ledbetter began a collaboration with T. Ogata to develop a low-temperature high-magnetic-field sound-velocity, elastic-constant apparatus.

Ohio State University

Vinod Tewary of Ohio State is a guest scientist working with R. D. Kriz on modelling interface problems related to the fracture of composite materials.

Osaka University

H. Ledbetter began a joint study with Y. Tsunoda (Physics Department) on the low-temperature elastic constants of copper containing gamma-iron particles.

A. V. Clark works with H. Fukuoka and M. Hirao on the development of ultrasonic measurement techniques for determining residual stress and texture.

Stanford University

A. V. Clark and P. J. Shull collaborate with B. A. Auld on capacitive array research.

C. M. Fortunko is collaborating with Professor B. T. Kuri-Yakub on the development of air-coupled ultrasonic transducers.

Tohoku University

H. Ledbetter collaborates with Y. Shindo of the Mechanical Engineering Faculty on problems of waves scattered by interfaces. They use a scattered-plane-wave ensemble-average model.

H. Ledbetter collaborates with M. Taya on problems of elastic constants of and internal strain (residual stress) in composites.

Tsinghua University

H. Ledbetter continues studies with Y. He (Physics Department): the behavior of low-temperature elastic constants and internal friction of metal-oxide superconductors.

University of Arkansas

H. Ledbetter collaborates with A. Hermann (Physics Department) on the physical properties of the new high-critical-temperature metal-oxide superconductors.

University of Belgrade

D. Mitraković was a guest worker at NIST in the Nondestructive Evaluation group, working on instrumentation for inspecting railroad wheels.

University of California

H. Ledbetter continues to work with J. Glazer and J. W. Morris, Jr. in studying the low-temperature elastic constants of an Al–Li alloy.

H. Ledbetter works with R. Fisher (Chemistry) to study specific heat of oxide superconductors.

University of Colorado

H. Ledbetter collaborates with Professor S. Datta (Mechanical Engineering Department) on theoretical problems of waves in heterogeneous media. They recently published several joint studies.

University of Geneva

H. Ledbetter continues studies with B. Seeber on the elastic constants of Chevrel-phase superconductors.

University of Hawaii

H. Ledbetter collaborates with M. Manghnani (Geophysics) to study pressure dependence of elastic constants of oxide superconductors.

University of Maryland

H. Ledbetter collaborates with R. Reno (Physics Department) on studies of the effects of texture on elastic constants.

J. R. Berger collaborates with J. W. Dally and R. J. Sanford (Mechanical Engineering Department) on studies of dynamic fracture and crack arrest in structural steels.

University of Michigan

D. W. Fitting is collaborating with researchers at the University of Michigan on the development of silicon-based acoustical arrays.

University of South Carolina

H. Ledbetter collaborates with T. Datta (Physics Department) on theoretical and experimental studies of low-temperature austenitic-steel physical properties, especially elastic constants and magnetic susceptibility.

University of Stuttgart

H. Ledbetter collaborates with E. Kröner and B. Gairola (Institute for Theoretical and Applied Physics) on theoretical problems of the elastic constants of polycrystals.

University of Tsukuba

H. Ledbetter collaborates with T. Suzuki (Applied Physics) on both theory and experiment of elastic constants and phase transitions. With K. Otsuka (Materials Science), H. Ledbetter studies the elastic constants of the monocrystal shape-memory alloy Cu–Al–Ni.

With M. Saito (Engineering Mechanics), H. Ledbetter studies problems of wave propagation in solids.

APPENDIX

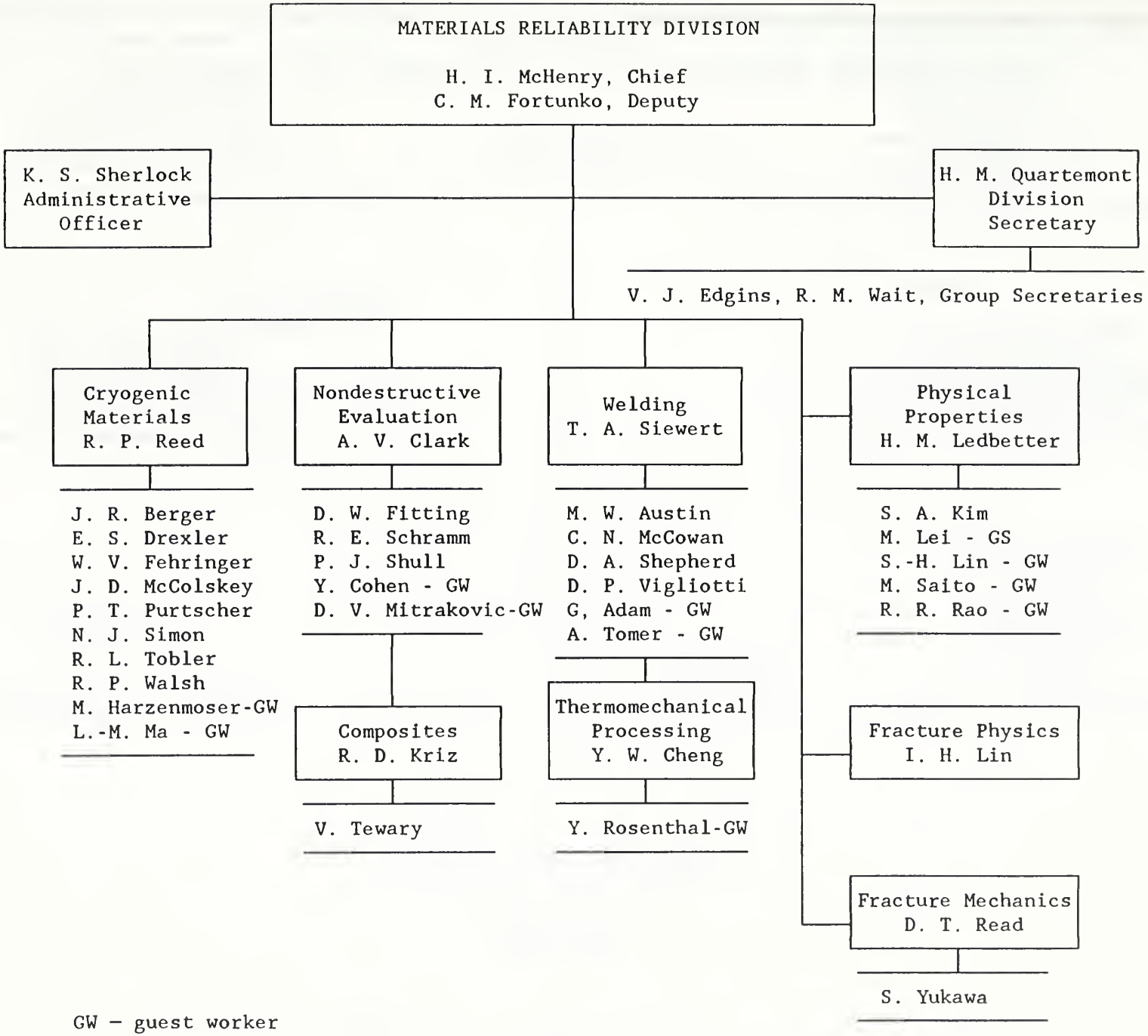

GW – guest worker
GS – graduate student

U.S. DEPARTMENT OF COMMERCE
National Institute of Standards and Technology

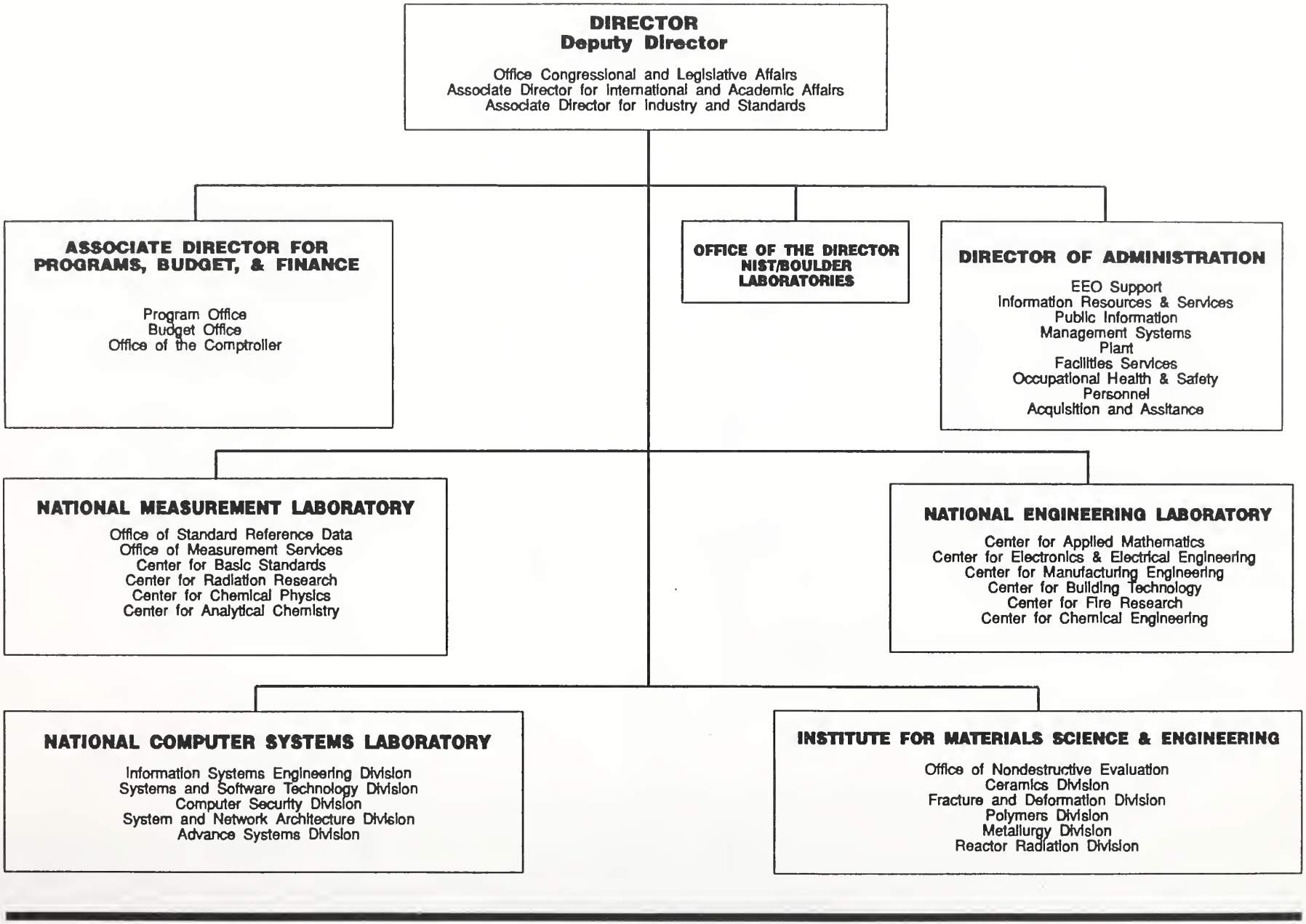

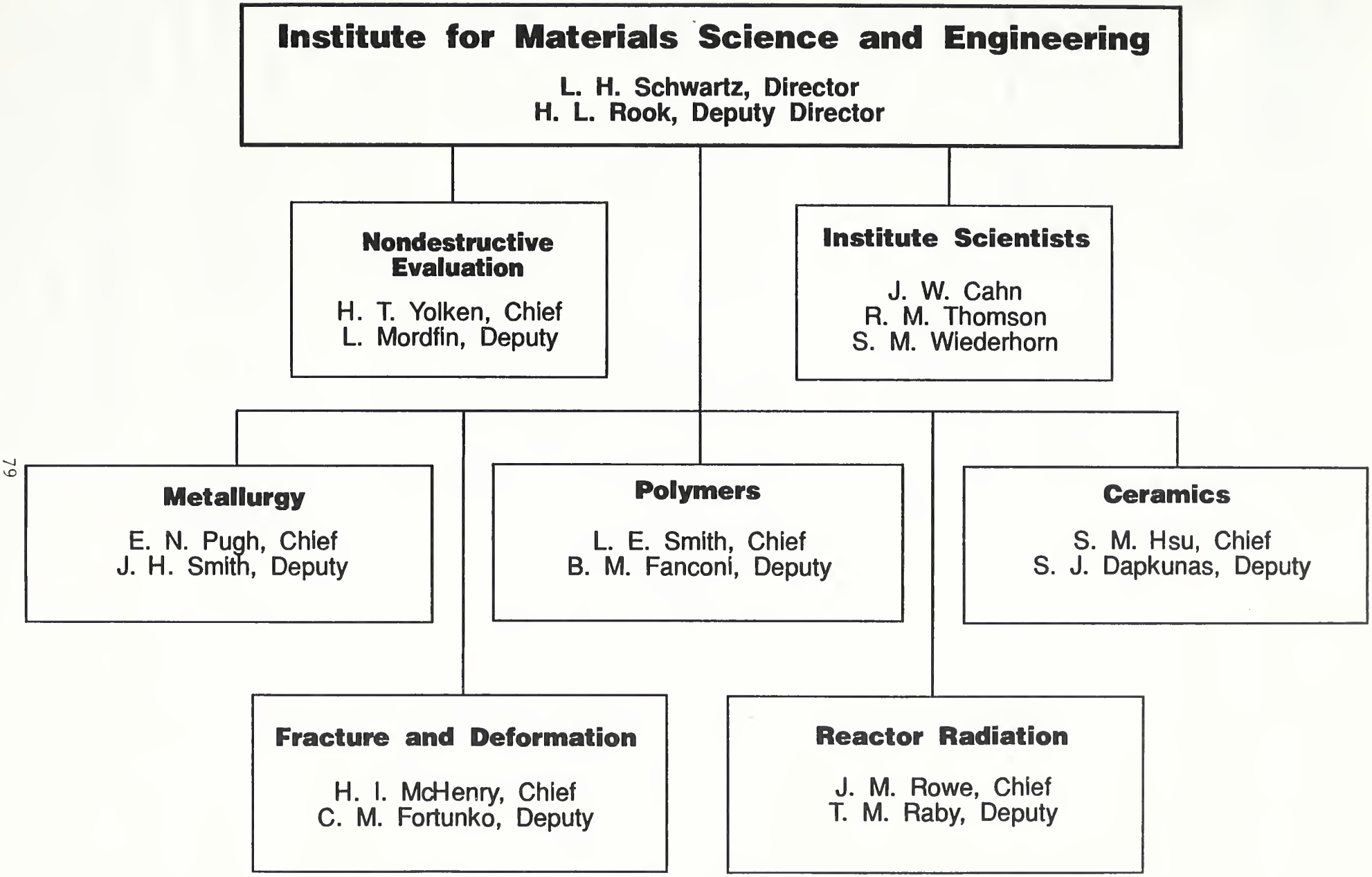
Institute for Materials Science and Engineering
L. H. Schwartz, Director
H. L. Rook, Deputy Director
Nondestructive Evaluation
H. T. Yolken, Chief
L. Mordfin, Deputy
Institute Scientists
J. W. Cahn
R. M. Thomson
S. M. Wiederhorn
Metallurgy
E. N. Pugh, Chief
J. H. Smith, Deputy
Polymers
L. E. Smith, Chief
B. M. Fanconi, Deputy
Ceramics
S. M. Hsu, Chief
S. J. Dapkunas, Deputy
Fracture and Deformation
H. I. McHenry, Chief
C. M. Fortunko, Deputy
Reactor Radiation
J. M. Rowe, Chief
T. M. Raby, Deputy

NBS-114A (REV. 2-8C)

U.S. DEPT. OF COMM. BIBLIOGRAPHIC DATA SHEET (See instructions)	1. PUBLICATION OR REPORT NO. NISTIR 89-4149	2. Performing Organ. Report No. B90-0048	3. Publication Date DECEMBER 1989

4. TITLE AND SUBTITLE

Institute for Materials Science and Engineering
Materials Reliability Division
Technical Activities 1989

5. AUTHOR(S)

H.I. McHenry, Editor

6. PERFORMING ORGANIZATION (If joint or other than NBS, see instructions)

NATIONAL BUREAU OF STANDARDS
DEPARTMENT OF COMMERCE
WASHINGTON, D.C. 20234

Early assignment of NISTIR No. 89-4149

7. Contract/Grant No.

8. Type of Report & Period Covered

9. SPONSORING ORGANIZATION NAME AND COMPLETE ADDRESS (Street, City, State, ZIP)

Materials Reliability Division, 430
National Institute of Standards and Technology
325 Broadway
Boulder, CO 80303

10. SUPPLEMENTARY NOTES

☐ Document describes a computer program; SF-185, FIPS Software Summary, is attached.

11. ABSTRACT (A 200-word or less factual summary of most significant information. If document includes a significant bibliography or literature survey, mention it here)

This report describes the 1989 fiscal-year programs of the Materials Reliability Division of the Institute for Materials Science and Engineering. It summarizes the principal accomplishments in three general research areas: materials performance, properties, and processing. The Fracture Mechanics, Fracture Physics, Nondestructive Evaluation, and Composite Materials Groups work together to detect damage in metals and composite materials and to assess the significance of the damage with respect to service performance. The Cryogenic Materials and Physical Properties Groups investigate the behavior of materials at low temperature and measure and model the physical properties of advanced materials, including composites, ceramics and the new high-critical-temperature superconductors. The Welding and Thermomechanical Processing Groups investigate the nonequilibrium metallurgical changes that occur during processing and affect the quality, microstructure, properties and performance of metals.

The report lists the division's professional staff, their research areas, publications, leadership in professional societies, and collaboration in research programs with industries and universities.

12. KEY WORDS (Six to twelve entries; alphabetical order; capitalize only proper names; and separate key words by semicolons)

composites; cryogenic materials; deformation; fracture; metallurgy; nondestructive evaluation; physical properties; steels; thermomechanical processing; welding

13. AVAILABILITY

☒ Unlimited
☐ For Official Distribution. Do Not Release to NTIS
☐ Order From Superintendent of Documents, U.S. Government Printing Office, Washington, D.C. 20402.
☒ Order From National Technical Information Service (NTIS), Springfield, VA. 22161

14. NO. OF PRINTED PAGES

83

15. Price

A05

USCOMM-DC 6043-P80